



Functional trait variation related to gap dynamics in tropical moist forests: a vegetation modelling perspective

Article

Accepted Version

Creative Commons: Attribution-Noncommercial-No Derivative Works 4.0

Togashi, H. F., Atkin, O. K., Bloomfield, K. J., Bradford, M., Cao, K., Dong, N., Evans, B. J., Fan, Z., Harrison, S. P., Hua, Z., Liddell, M. J., Lloyd, J., Ni, J., Wang, H., Weerasinghe, L. K. and Prentice, I. C. (2018) Functional trait variation related to gap dynamics in tropical moist forests: a vegetation modelling perspective. *Perspectives in Plant Ecology, Evolution and Systematics*, 35. pp. 52-64. ISSN 1433-8319 doi: <https://doi.org/10.1016/j.ppees.2018.10.004> Available at <http://centaur.reading.ac.uk/80295/>

It is advisable to refer to the publisher's version if you intend to cite from the work. See [Guidance on citing](#).

To link to this article DOI: <http://dx.doi.org/10.1016/j.ppees.2018.10.004>

Publisher: Elsevier

All outputs in CentAUR are protected by Intellectual Property Rights law, including copyright law. Copyright and IPR is retained by the creators or other copyright holders. Terms and conditions for use of this material are defined in the [End User Agreement](#).

www.reading.ac.uk/centaur

CentAUR

Central Archive at the University of Reading

Reading's research outputs online

1 **Functional trait variation related to gap dynamics in tropical moist forests: a**
2 **vegetation modelling perspective**

3

4 Henrique Fürstenau Togashi^{a,b,*}, Owen K. Atkin^{c,d}, Keith J. Bloomfield^c, Matt
5 Bradford^e, Kunfang Cao^f, Ning Dong^{a,b,g}, Bradley J. Evans^{a,b}, Zexin Fan^h, Sandy P.
6 Harrison^{a,g}, Zhu Hua^h, Michael J. Liddellⁱ, Jon Lloyd^{i,j}, Jian Ni^{k,l}, Han Wang^{a,m},
7 Lasantha K. Weerasinghe^{c,n}, Iain Colin Prentice^{a,j,m,o}

8

9 ^aDepartment of Biological Sciences, Macquarie University, North Ryde, NSW 2109,
10 Australia

11 ^bThe Ecosystem Modelling and Scaling Infrastructure Facility (eMAST), Faculty of
12 Agriculture and Environment, Department of Environmental Sciences, The University
13 of Sydney, NSW 2006, Australia

14 ^cDivision of Plant Sciences, Research School of Biology, Australian National
15 University, Canberra, ACT 2601, Australia

16 ^dARC Centre of Excellence in Plant Energy Biology, Research School of Biology,
17 Australian National University, Canberra, ACT 2601, Australia

18 ^eCommonwealth Science and Industrial Research Organization (CSIRO), Tropical
19 Forest Research Centre, Atherton, Queensland 4883, Australia

20 ^fState Key Laboratory of Conservation and Utilization of Subtropical Agro-
21 bioresources, College of Forestry, Guangxi University, Daxuedonglu 100, Nanning
22 530005, Guangxi, China

23 ^gSchool of Archaeology, Geography and Environmental Sciences, University of
24 Reading, Whiteknights, Reading RG6 6AB, UK

25 ^hKey Laboratory of Tropical Forest Ecology, Xishuangbanna Tropical Botanical
26 Garden, Chinese Academy of Sciences, Menglun, Mengla, Yunnan 666303, China

27 ⁱCentre for Tropical Environmental and Sustainability Science (TESS) and College of
28 Science, Technology and Engineering, James Cook University, Cairns, Queensland
29 4878, Australia

30 ^jDepartment of Life Sciences, Imperial College London, Silwood Park Campus,
31 Buckhurst Road, Ascot SL5 7PY, UK

32 ^kState Key Laboratory of Environmental Geochemistry, 99 Lincheng West Road,
33 Guanshanhu, Guiyang, Guizhou 550081, China

34 ^lCollege of Chemistry and Life Sciences, Zhejiang Normal University, Yingbin
35 Avenue 688, Jinhua 321004, Zhejiang, China

36 ^mDepartment of Earth System Science, Tsinghua University, Beijing 100084, China

37 ⁿFaculty of Agriculture, University of Peradeniya, Peradeniya 20400, Sri Lanka

38 ^oState Key Laboratory of Soil Erosion and Dryland Farming on the Loess Plateau,
39 College of Forestry, Northwest Agriculture & Forestry University, Yangling 712100,
40 China

41

42 *Corresponding author (henriquetogashi@gmail.com)

43

44 ABSTRACT

45 The conventional representation of Plant Functional Types (PFTs) in Dynamic Global
46 Vegetation Models (DGVMs) is increasingly recognized as simplistic and lacking in
47 predictive power. Key ecophysiological traits, including photosynthetic parameters,
48 are typically assigned single values for each PFT while the substantial trait variation
49 within PFTs is neglected. This includes continuous variation in response to
50 environmental factors, and differences linked to spatial and temporal niche
51 differentiation within communities. A much stronger empirical basis is required for
52 the treatment of continuous plant functional trait variation in DGVMs. We analyse
53 431 sets of measurements of leaf and plant traits, including photosynthetic
54 measurements, on evergreen angiosperm trees in tropical moist forests of Australia
55 and China. Confining attention to tropical moist forests, our analysis identifies trait
56 differences that are linked to vegetation dynamic roles. Coordination theory predicts
57 that Rubisco- and electron-transport limited rates of photosynthesis are co-limiting
58 under field conditions. The least-cost hypothesis predicts that air-to-leaf CO₂
59 drawdown minimizes the combined costs per unit carbon assimilation of maintaining
60 carboxylation and transpiration capacities. Aspects of these predictions are supported
61 for within-community trait variation linked to canopy position, just as they are for
62 variation along spatial environmental gradients. Trait differences among plant species
63 occupying different structural and temporal niches may provide a basis for the
64 ecophysiological representation of vegetation dynamics in next-generation DGVMs.

65

66 Keywords: plant traits, photosynthesis, vegetation dynamics, tropical forests, DGVMs

67 **Introduction**

68 The development of Dynamic Global Vegetation Models (DGVMs) from the
69 earliest stages has emphasized the role of the distribution of different types of plants
70 and vegetation in predicting the exchanges of carbon between the atmosphere and the
71 land biota (Prentice et al., 2007; Prentice and Cowling, 2013). Plant Functional Type
72 (PFT) classifications can be traced back to the Raunkiær's (1934) 'life form'
73 classification, based on plant traits that ensure persistence through seasons
74 unfavourable for growth (Harrison et al., 2010). After several decades during which
75 plant functional geography was neglected, new PFT classifications appeared during
76 the 1980s (Box, 1981; Woodward, 1987) with a view to the development of DGVMs
77 – which began in earnest during the late 1980s. The PFT concept has received
78 significant attention since then (Prentice et al., 1992; Díaz and Cabido, 1997; Lavorel
79 and Garnier, 2002; Wright et al., 2004; Prentice et al., 2007; Harrison et al., 2010;
80 Fyllas et al., 2012). It has become widely accepted that PFT classifications for
81 modelling purposes ideally should reflect aspects of trait diversity that can predict
82 plant responses to the physical environment.

83 PFTs adopted in DGVMs today are commonly defined in terms of up to five
84 qualitative traits: (a) life form, (b) leaf type, (c) phenological type, (d) photosynthetic
85 pathway and (e) climatic range defined in terms of broad climatic classes such as
86 'boreal' and 'tropical'. This conventional approach to PFT classification has manifold
87 limitations (Prentice and Cowling, 2013). For example, life-forms are often
88 incompletely defined in functional terms. Informal and potentially ambiguous terms
89 such as 'shrub' have been used in place of Raunkiær's explicit functional categories.
90 Leaf-type definitions usually ignore the huge variations in leaf size and shape among
91 'broad-leaved' plants. Even the distinction between broad and needle-leaved trees is
92 often effectively an imperfect surrogate for the important distinction in hydraulic
93 architecture between angiosperms and gymnosperms – the latter, in fact, including
94 many species with broad leaves. Thermal climate categories may make sense if they
95 are recognized as a surrogate for different cold-tolerance mechanisms in
96 phanerophytes (Prentice et al., 1992). Harrison et al. (2010) provided a more recent
97 compilation of experimental data on cold tolerance. However, such categories are
98 often used without clear definitions. They may stand in for a continuum of
99 physiological differences between plants adapted or acclimated to different seasonal

100 temperature regimes, rather than representing qualitative differences among distinct
101 types of plant. Moreover, thermal climate categories may artificially restrict modelled
102 PFT distributions within confined areas even if the absence of a given PFT from a
103 wider area could be due to competitive exclusion by other types. Ideally, shifts of
104 dominance in models should not be imposed in this way, but should emerge naturally
105 through competitive advantage (Fisher et al., 2015).

106 A distinct aspect of plant functional classification pertains to species' 'roles'
107 in vegetation dynamics. Classifications of tree species according to shade tolerance
108 (Whitmore, 1982), growth characteristics: maximum height and growth rate (Shugart,
109 1984; Swaine and Whitmore, 1988) and successional stage (pioneer *versus* climax)
110 Swaine and Whitmore (1988) have been a mainstay of regionally specific 'gap
111 models' designed to predict forest dynamics under constant or changing
112 environmental conditions (Botkin et al., 1972; Shugart, 1984; Denslow, 1987;
113 Prentice and Leemans, 1990; Prentice et al., 1993; Turner, 2001) but are not treated
114 by most DGVMs. Exceptions are those models with individual-based dynamical
115 cores, such as LPJ-GUESS (Smith et al., 2001), Hybrid (Friend et al., 1993), ED
116 (Moorcroft et al., 2001; Medvigy et al., 2009), aDGVM2 (Langan et al., 2017), and
117 models that make use of the Perfect Plasticity Approximation (PPA). PPA is a
118 mathematical approach designed to represent the essentials of forest dynamics
119 without simulating individual trees explicitly (Purves et al., 2008; Fyllas et al., 2014;
120 Fisher et al., 2015).

121 A general critique of the use of PFTs for modelling purposes has emerged
122 with the development of new dynamic vegetation models based on continuous trait
123 variation (Pavlick et al., 2013; Scheiter et al., 2013; Verheijen et al., 2013; Fyllas et
124 al., 2014; van Bodegom et al., 2014; Sakschewski et al., 2015), raising a question as
125 to whether distinct PFTs are necessary for modelling vegetation. In our view there is a
126 clear-cut case for retaining the well-understood distinctions among photosynthetic
127 pathways, and there may also be good reasons also to retain life-form distinctions – at
128 least at the highest level of Raunkiaer's classification. However, most quantitative
129 traits show continuous adaptive variation along environmental gradients (Meng et al.,
130 2015), indicating that the conventional approach of assigning fixed values of leaf-
131 level traits such as carboxylation capacity (V_{cmax}) and nitrogen content per unit leaf
132 area (N_{area}) to PFTs does not adequately describe the plasticity of such traits within
133 species (phenotypic plasticity). Even biophysical traits such as leaf mass per area

134 (LMA) and leaf dry-matter content, which are typically less plastic than metabolic
135 traits (Meng et al., 2015; Dong et al., 2017), show systematic, quantitative variations
136 along environmental gradients, partly as a consequence of species turnover within
137 PFTs and thus not necessarily the replacement of one PFT by another. Faced with
138 continuous trait variation (due to species or genotypic turnover and/or phenotypic
139 plasticity), models can either treat it as continuous – as the LPJ DGVM (Sitch et al.,
140 2003) does for photosynthetic traits, following the approach developed by Haxeltine
141 and Prentice (1996) – or subdivide the continuum into arbitrary sections. However,
142 problems such as unrealistically abrupt modelled vegetation transitions can arise if the
143 subdivision of the continuum is too coarse, suggesting that a continuous
144 representation will be more useful.

145 This paper describes an empirical analysis that is oriented towards the
146 improvement of DGVMs. Our primary focus is on the largely neglected ‘dynamical’
147 aspect of PFT classification. We adopt the fourfold scheme introduced by Shugart
148 (1984) as an initial scheme to classify species’ dynamic roles. We recognize that this
149 classification represents a subdivision of two orthogonal continua of variation: shade
150 tolerance (requiring, *versus* not requiring, a gap for regeneration) and size at maturity
151 (producing, *versus* not producing, a gap upon mortality). We focus on functional trait
152 variations within tropical moist forests, which harbour enormous tree species diversity
153 and contain species that exhibit all combinations of these traits (Turner, 2001). We
154 build on a previous analysis by Fyllas et al. (2012), who showed that quantitative
155 traits including foliar $\delta^{13}\text{C}$ discrimination, LMA and nutrients including N and P
156 could be used to discriminate PFTs with distinct dynamic characteristics in
157 Amazonian rain forests. Our analysis focuses on east Asian (SW China) and northern
158 Australian tropical rain forests, and extends the approach of Fyllas et al. (2012) to
159 include field photosynthetic measurements.

160 **Theory and Principles**

161 Recent empirical analyses aiming to inform the development of ‘next-
162 generation’ DGVMs have focused on the predictability of key quantitative traits as a
163 function of environmental variation (Yang et al., 2018). The ‘least-cost’ (Prentice et
164 al., 2014) and ‘coordination’ (Maire et al., 2012) hypotheses together suggest a degree
165 of predictability for the air-to-leaf CO_2 drawdown (χ , the ratio of leaf-internal to

166 ambient CO₂) (Prentice et al., 2014; Wang et al., 2017), V_{cmax} and the electron-
167 transport capacity J_{max} (Togashi et al., 2017), and N_{area} (Dong et al., 2017) across
168 environments and clades. Both hypotheses have a much longer pedigree than
169 indicated by the recent references cited here, but systematic testing of these
170 hypotheses has only been undertaken quite recently.

171 The least-cost hypothesis proposes that at the leaf level, plants should respond
172 to differences in the relative costs (per unit of assimilation achieved) of maintaining
173 the biochemical capacity for photosynthesis *versus* the structural capacity for
174 transpiration by making an optimal investment ‘decision’ that minimizes the total
175 carbon cost of maintaining both essential functions. This hypothesis can be shown to
176 lead to an optimum value of χ that depends predictably on temperature, vapour
177 pressure deficit and atmospheric pressure (Prentice et al., 2014; Wang et al., 2017).
178 The mathematical expression of this optimum value includes a parameter that is
179 influenced by low plant-available moisture, and therefore by soil moisture and rooting
180 characteristics (Zhou et al., 2013). This optimum has the same mathematical form as
181 that predicted approximately by the Cowan-Farquhar optimality criterion for electron-
182 transport limited photosynthesis. This form is known to provide good predictions of
183 stomatal behaviour under a range of conditions (Medlyn et al., 2011; Lin et al., 2015;
184 Dewar et al., 2018). The least-cost hypothesis however is more explicit than the
185 Cowan-Farquhar criterion in that it ‘unpacks’ water transport and biochemical costs,
186 and assigns to each of them an explicit ecophysiological meaning.

187 The coordination hypothesis indicates that under typical daytime conditions,
188 the Rubisco-limited and electron transport-limited rates of photosynthesis should be
189 approximately equal (Chen et al., 1993; Haxeltine and Prentice, 1996; Maire et al.,
190 2012). This represents the optimal disposition of resources between light capture and
191 carbon fixation. It leads to the prediction that the outer-canopy V_{cmax} measured at the
192 prevailing growth temperature should be determined by χ (higher values of one
193 quantity are consistent with lower values of the other), temperature (higher V_{cmax} is
194 required to achieve a given assimilation rate at higher temperatures), and incident
195 photosynthetically active radiation (PAR) (productive investment in V_{cmax} is directly
196 proportional to the available PAR) (Dong et al., 2017). N_{area} is generally found to be
197 roughly linearly related to Rubisco content, and thus to V_{cmax} at standard temperature.
198 However, leaf N also has structural and defensive components that are roughly
199 proportional to LMA and represent a largely independent source of variation in N_{area}

200 (Dong et al., 2017). So far, these predictions have been supported for seasonal
201 variations within individual plants (Togashi et al., 2017), and for spatial variations
202 along environmental gradients (Prentice et al., 2014; Dong et al., 2017). Here we
203 extend their application to biotically conditioned, microenvironmental variation
204 within forest environments. The framework provided by the least-cost and
205 coordination hypotheses suggest moreover that shade tolerance, and stem properties
206 such as height and wood density, should also be related to leaf metabolic and
207 structural traits, as proposed by Whitehead et al. (1984) and many later commentators.

208 The least-cost and coordination hypotheses are optimality concepts, whose
209 rationale depends on the heuristic principle that natural selection is expected to have
210 eliminated all trait combinations that fall short of optimality according to some
211 specified criterion. Another optimality concept lies behind the Leaf Economics
212 Spectrum, LES (Wright et al., 2004). Fundamentally, the LES represents a universal
213 negative correlation between LMA and leaf life-span (Lloyd et al., 2013), which can
214 be considered to arise from a trade-off because (a) carbon available for investment in
215 leaves is limited and (b) long-lived leaves need to be thicker and/or tougher than
216 short-lived leaves in order to avoid high risks of predation by herbivores and other
217 kinds of mechanical damage. Thus leaves can be short-lived and flimsy or long-lived
218 and thick and/or tough, or somewhere in between. In contrast, short-lived leaves with
219 high LMA would be uneconomic, while long-lived leaves with low LMA would be
220 unviable.

221 In this study we consider four groups of leaf and stem traits. The first group
222 consists of leaf metabolic traits: V_{cmax} , J_{max} and leaf dark respiration (R_{dark}), which has
223 been found to correlate with V_{cmax} (Atkin et al., 2000; Weerasinghe et al., 2014). The
224 second group contains the leaf structural/chemical traits N_{area} , P_{area} and LMA. As
225 previously noted, N_{area} has a metabolic component as well as a structural component,
226 and the same may be true for P_{area} (Evans, 1989; Reich et al., 1997; Fyllas et al.,
227 2009). But increasing evidence points to the dominance of the structural component
228 when large sets of species are considered (Dong et al., 2017; Yang et al., 2018). The
229 third group, represented principally by wood density (WD), stands in for plant
230 hydraulics: denser wood tends to have lower permeability to water (Sperry, 2003; Lin
231 et al., 2015). Wood density also directly influences plant growth because volume
232 growth is necessarily slower, for a given photosynthetic output, in trees with dense
233 wood. Relatively more carbon also needs to be allocated to high-density wood, at the

234 expense of allocation to leaves and fine roots. Although the correlation between WD
235 and more directly instrumental traits for plant hydraulics, such as the Huber value (the
236 ratio of cross-sectional sapwood area to subtended leaf area) (Togashi et al., 2015),
237 vessel density and calibre, and permeability (Reid et al., 2005) is imperfect, these last
238 traits are much more time-consuming to measure than WD and thus comparatively
239 under-represented in available data sets. We anticipate that plants with a lavish water
240 use strategy should present high conductivity and low-density wood, while plants
241 adapted to environments with long droughts, or vulnerable to water use competition,
242 should tend to adopt a conservative water-use strategy and to have high-density wood.
243 The fourth group reflects the ability to compete with other species for light, expressed
244 as potential maximum height (H_{\max}): taller plants are able to harvest more light while
245 shorter plants are often more shade-tolerant (Turner, 2001). This group includes χ ,
246 which has been reported to show a negative relationship with tree height (Koch et al.,
247 2015). The reason χ belongs with H_{\max} and not with V_{cmax} in this analysis is because
248 we have intentionally restricted the climatic range to moist forests, so that the
249 variation in χ is mainly related to plant strategy rather than to aridity or temperature.
250 H_{\max} is considered to be a species characteristic and although it may not be reached at
251 every site, its use as an indicator of plant strategy is likely better than using actual
252 observed height, which varies among individuals and over time.

253 Leaf-level measurements were conducted in tropical forests of Queensland,
254 Australia and Yunnan, China, and combined with (a) published and unpublished
255 datasets on H_{\max} , WD, and (b) expert knowledge of the species' vegetation dynamical
256 roles (climax, subcanopy, large and small pioneers). Thus we are able to present what
257 is (to our knowledge) the first study to analyse key biochemical rates in the context of
258 tree species' contrasting dynamic roles, and the first empirical trait-based analysis to
259 include measured biochemical rates in a PFT classification with the aim to inform
260 progress in DGVM development. The objective of this work was to quantify trait
261 variation within these forests that can be linked to dynamical roles, but also
262 specifically to test the following predictions: (i) when moisture supply and low
263 temperatures are not limiting factors, photosynthetic capacity should be governed by
264 incident PAR (a prediction of the coordination hypothesis); (ii) χ should be lower at
265 high H_{\max} (a prediction of the least-cost hypothesis); and (iii) pioneer species should

266 tend to have low WD, an expectation from the theory of forest dynamics (Shugart,
267 1984).

268 **Materials and methods**

269 **Study Sites**

270 Our analysis includes material from 232 evergreen angiosperm tree species
271 (431 leaf samples) from moist tropical forests of Queensland, northern Australia
272 (Robson Creek on the inland Atherton Tablelands to Cape Tribulation near the Pacific
273 coast) and Yunnan, southwestern China (the Xishuangbanna region in southern
274 Yunnan, near the land borders with Myanmar, Thailand and Laos). Field campaigns
275 conducted in Queensland and Yunnan yielded data on 191 species. Data from these
276 campaigns were combined with data on a further 41 Queensland species from field
277 studies carried out by the TROpical Biomes In Transition (TROBIT) network
278 (Bloomfield et al., 2014). Climates covered by the sampled areas range in mean
279 annual precipitation (MAP) from 1427 to 5143 mm (Liddell, 2013b, a; Harris et al.,
280 2014; Hutchinson, 2014c) and in mean annual temperature (MAT) between 19.0 and
281 24.4 °C (Liddell, 2013b, a; Harris et al., 2014; Hutchinson, 2014a, b). Both
282 Queensland and Yunnan have a marked wet season and ‘dry’ (drier) season, and
283 although the range of MAP values is considerable, all the sites correspond to climates
284 where moisture is unlikely to be a limiting factor for forest development. The drier
285 season at the Queensland and Yunnan sites lasts four to five months, but there is still
286 typically 100-300 mm precipitation per month. Gridded climatological data at 0.01°
287 resolution for 1971-2000 on MAP, MAT, annual Moisture Index (MI, the ratio of
288 precipitation to equilibrium evaporation) and mean monthly photosynthetic active
289 radiation (mPAR) were acquired for the Australian sites at www.tern.org.au.
290 Climatological data for the Chinese sites were derived from records at 1814
291 meteorological stations (740 stations have observations from 1971-2000, the rest from
292 1981-1990: China Meteorological Administration, unpublished data), interpolated to a
293 0.01° grid using a three dimensional thin-plate spline (ANUSPLIN version 4.36,
294 Hancock and Hutchinson, 2006). Fig. 1 and Table 1 provide further details on sites
295 and climates.

296 **Gas exchange measurements and photosynthetic variables**

297 We used a portable infrared gas analyser (IRGA) system (LI-6400; Li-Cor,
298 Inc., Lincoln, NB, USA) to perform leaf gas-exchange measurements. Sunlit terminal
299 branches from the top one-third of the canopy were collected and immediately re-cut
300 under water. One of the youngest fully expanded leaves, attached to the branch, was
301 sealed in the leaf chamber. Measurements in the field were taken with relative
302 humidity and chamber block temperature close to those of the ambient air at the time
303 of measurement. The rate of airflow was held constant at 500 $\mu\text{mol s}^{-1}$, but
304 exceptionally the flow was reduced (to a minimum of 250 $\mu\text{mol s}^{-1}$) under very low
305 stomatal conductance.

306 We obtained 130 $A-c_i$ curves from 41 species from Robson Creek (*RCR1* and
307 *RCR2*) in both the dry and the wet season. The CO_2 mixing ratios for the $A-c_i$ curves
308 proceeded stepwise down from 400 to 35 and up to 2000 $\mu\text{mol mol}^{-1}$. Prior to the
309 measurements, we tested plants to determine appropriate light-saturation levels. The
310 photosynthetic photon flux density (PPFD) adopted for measurement ranged between
311 1500 and 1800 $\mu\text{mol m}^{-2} \text{s}^{-1}$. After measuring the $A-c_i$ curves over about 35 minutes,
312 light was set to zero for five minutes before measuring respiration. This was a time-
313 saving compromise to allow four or five replicate curves per machine per day, based
314 on our experience that stable results are commonly obtained after five minutes.
315 Moreover, this quick estimate should be superior to the common practice of deriving
316 R_{dark} as one of the parameters in a curve-fitting routine. Following the protocol of
317 Domingues et al. (2010), we discarded 37 of a total 167 $A-c_i$ curves in which stomatal
318 conductance (g_s) declined to very low levels, adversely affecting the calculation of
319 V_{cmax} . These procedures were very similar to the ones applied to the 125 $A-c_i$ curves
320 obtained from 26 species in the TROBIT sites (*CTR2*, *KBL1*, *KBL3* and *KCR*) during
321 the wet season, further described in Bloomfield et al. (2014).

322 We sampled 114 leaves of 91 species in Yunnan (*Y1X*, *Y2U*, *Y3M1*, *Y3M2*,
323 *Y4L*) in the dry season. Data for 62 leaves of 16 species were also obtained from Cape
324 Tribulation in the dry season (*CTR1*; Weerasinghe et al., 2014). We used the same
325 sampling methods for Yunnan and for Cape Tribulation. PPFD was held constant at
326 1800 $\mu\text{mol m}^{-2} \text{s}^{-1}$. For each leaf, we first set the CO_2 mixing ratio to 400 $\mu\text{mol mol}^{-1}$
327 to obtain the rate of photosynthesis under light saturation (A_{sat}). Measurement was
328 taken under stable g_s ($> 0.5 \mu\text{mol m}^{-2} \text{s}^{-1}$), CO_2 and leaf-to-air vapour pressure deficit.

329 The next step was to increase the CO₂ mixing ratio to 2000 μmol mol⁻¹ in order to
330 register the rate of photosynthesis under light and CO₂ saturation (A_{\max}). R_{dark} was not
331 measured in Yunnan. For R_{dark} in *CTRL*, the leaf was wrapped in foil sheets after A_{sat}
332 and A_{\max} measurements. There was a waiting period of at least 30 minutes of darkness
333 before taking R_{dark} values.

334 Values of V_{cmax} and J_{max} were fitted using the Farquhar et al. (1980) model.
335 The assumption of unlimited mesophyll conductance (Miyazawa and Kikuzawa,
336 2006; Lin et al., 2013) remains the standard implementation of the Farquhar model
337 although it is recognized to be an approximation that results in an overestimation of
338 V_{cmax} and J_{max} . Hence all of the values estimated are ‘apparent’ V_{cmax} and J_{max} values,
339 as in most of the ecophysiological literature. In cases where A - c_i curves were not
340 measured, we estimated V_{cmax} from A_{sat} by the so-called one-point method, which
341 inverts the equation for Rubisco-limited photosynthesis taking into account the
342 measured c_i and leaf temperature by applying the temperature dependencies of the
343 Michaelis-Menten coefficients of Rubisco for carboxylation (K_C) and oxygenation
344 (K_O) and the photorespiratory compensation point (Γ^*) from Bernacchi et al. (2001).
345 The one-point method relies on the assumption that light-saturated photosynthesis
346 measured on field-grown plants is Rubisco-limited, which has been found to be true
347 in almost all cases (De Kauwe et al., 2016). J_{max} was estimated from A_{max} on the
348 assumption that high CO₂ forces the leaves into electron-transport limitation
349 (Bernacchi et al., 2003). Triose phosphate utilization limitation was not considered, as
350 it would be unlikely to occur at our field temperatures > 22 °C (Sharkey et al., 2007;
351 Lombardozzi et al., 2018)

352 **Nutrient analyses**

353 After completion of the leaf gas-exchange measurements, the leaf was retained
354 to determine leaf area, dry mass, and mass-based N and P concentrations (N_{mass} and
355 P_{mass} , mg g⁻¹). Leaves were sealed in plastic bags containing moist tissue paper to
356 prevent wilting. Leaf area was determined using a 600 dot/inch flatbed top-
357 illuminated optical scanner and Image J software (<http://imagej.nih.gov/ij/>). Leaves
358 were dried in a portable desiccator for 48 hours for preservation until the end of the
359 campaign and subsequently oven-dried in the laboratory for 24 hours at 70°C. Then
360 the dry weight was determined (Mettler-Toledo Ltd, Port Melbourne, Victoria,

361 Australia). LMA (g m^{-2}) was calculated from leaf area and dry mass. N_{mass} and P_{mass}
362 were obtained by Kjeldahl acid digestion of the same leaves (Allen et al., 1974). The
363 leaf material was digested using 98% sulphuric acid and 30% hydrogen peroxide.
364 Digested material was analyzed for N and P using a flow injection analyser system
365 (LaChat QuikChem 8500 Series 2, Lachat Instruments, Milwaukee, WI, USA). N_{area}
366 and P_{area} (mg m^{-2}) were calculated as products of LMA and N_{mass} or P_{mass} . TROBIT
367 nutrient analysis was performed using similar methods but different equipment, as
368 described in Bloomfield et al. (2014).

369 **Wood density and tree height**

370 Twenty-year series of wood density (WD), tree height (H), and tree diameter
371 at breast height (D) were obtained from Bradford et al. (2014a) ($n = 138$). Maximum
372 tree height (H_{max}) was estimated using the derivative of the Mitscherlich function
373 relating diameter and height (Li et al., 2014):

$$374 \quad \frac{dH}{dD} = a \exp(-aD/H_{\text{max}}) = a(1 - H/H_{\text{max}}) \quad (1)$$

375 where a is the initial slope of the relationship between height and diameter. A typical
376 range of a in the literature is 116 ± 4.35 .

377 **Dynamic roles of species**

378 Australian species ($n = 61$) were assigned to dynamic roles with the help of
379 the database published by Bradford et al. (2014b) and expert knowledge by MB.
380 Chinese species ($n = 85$) were assigned to dynamic roles based on expert knowledge
381 by ZH. These ‘expert’ classifications (A1) were compared with a quantitative trait-
382 based classification (A2) as described in the next section. Both classification
383 approaches were implemented according to the Shugart (1984) framework, which can
384 also be related to those of Denslow (1987), Turner (2001) and Fyllas et al. (2012):

385

386 (1) Requires a gap, and produces a gap. These are long-lived pioneers that reach the
387 canopy. Shade intolerant.

388 (2) Does not require a gap, but produces a gap. These are long-lived climax species
389 that reach the canopy and grow large. Shade tolerant.

390 (3) Requires a gap, but does not produce a gap. These are short-lived pioneers that
391 never grow large. Shade intolerant.

392 (4) Does not require a gap, and does not produce a gap. These are sub-canopy species.
393 Shade tolerant.

394

395 The geographic distribution of expert assessment of dynamic roles per number of
396 species and per number of leaves is shown in Table 2. This dataset includes 262
397 observations.

398 **Statistical analyses**

399 All statistics were performed in R (R Core Team, 2012). For graphing we used the
400 `ggplot2` package (Wickham, 2010). Moisture index was represented in Fig. 1 as its
401 square root, a transformation appropriate to precipitation values (M.F. Hutchinson,
402 personal communication, 2011), which approximately normalizes the distribution of
403 values and thus contains the large spread of values at the high end. V_{cmax} , J_{max} , R_{dark} ,
404 LMA, N_{area} , P_{area} , H_{max} and WD data were \log_{10} -transformed, unless otherwise
405 indicated, achieving an approximately normal distribution of values. χ was logit-
406 transformed as this variable is bounded between 0 and 1, and the logit transformation
407 results in approximately linear relationships between the transformed ratio and
408 environmental predictors, including temperature (Wang et al., 2017). Ordinary least-
409 squares linear regression was used to test relationships between plant traits and
410 climate variables. Pairwise combinations of quantitative traits were tested for
411 significant relationships across all data, and within groups corresponding to high and
412 low MI, high and low mPAR, and high and low MAT. Slopes and elevations of
413 regressions were compared using standardized major axis regression with the `smatr`
414 package (Warton et al., 2006). The package `vegan` (Oksanen et al., 2015) was used
415 to assess multivariate trait variation, using the following methods:

- 416 • Principal component analysis (PCA) of nine plant traits (V_{cmax} , J_{max} , R_{dark} ,
417 LMA, N_{area} , P_{area} , H_{max} , WD and χ);
- 418 • Redundancy analysis (RDA) of the same nine traits, constrained by three
419 climate variables (MI, mPAR and MAT);
- 420 • RDA of the same nine traits, constrained by dynamic roles (as factors); and

- 421 • RDA of the same nine traits constrained simultaneously by both climate and
422 dynamic roles.

423 PCA was used to identify patterns of covariation among traits irrespective of their
424 dynamic or environmental correlates, and RDA to analyse multivariate trait
425 relationships to predictors. Note that PCA is an exploratory method with no
426 associated formal test of significance. By contrast, the significance of trait-
427 environment relationships identified by RDA can be assessed approximately in a
428 similar way to generalized linear models (Ter Braak and Prentice, 1988). The *K*-
429 means (R Core Team, 2012) clustering method was used to create four groups of
430 species based on the nine plant traits (A2: Dynamic roles based on quantitative
431 assessment). *K*-means clustering was performed with the number of iterations set to
432 100 and bootstrapped with 10,000 repetitions. RDA and bivariate correlations were
433 used to compare classifications A2 and A1. The dataset used for PCA and RDA
434 analysis consisted of 130 observations with information for all traits, climate variables
435 and dynamic roles. All RDA visualizations here follow the response-variable focused
436 ‘Type 2 scaling’ (Oksanen et al., 2015), such that the angles between pairs of vectors
437 as plotted approximate their pairwise correlations. For PCA and RDA input data
438 where direct measurements of R_{dark} were not available, R_{dark} ($n = 58$) was estimated
439 from A_{sat} following Prentice et al. (2014) using the approximation $R_{\text{dark}} \approx 0.01 V_{\text{cmax}}$
440 (De Kauwe et al., 2016).

441 **Research data**

442 Robson Creek (*RCR1* and *RCR2*) data can be requested at www.tern.org.au
443 (Prentice et al., 2013). Access to TROBIT data (*CTR2*, *KBL1*, *KBL3* and *KCR*) and
444 Cape Tribulation 1 (*CTR1*) are described in Bloomfield et al. (2014) and Weerasinghe
445 et al. (2014) respectively. For Yunnan data (*Y1X*, *Y2U*, *Y3M1*, *Y3M2*, *Y4L*), refer to
446 Wang et al. (2018).

447

448 **Results**

449 **Trait values and dimensions of variation**

450 Average values of the metabolic traits V_{cmax} , J_{max} , and R_{dark} were 52.0, 82.0,
451 and $0.63 \mu\text{mol m}^{-2} \text{s}^{-1}$ respectively. The corresponding ranges were 4.2 to 148.9, 14.0

452 to 203.6, and near zero to $3.70 \mu\text{mol m}^{-2} \text{s}^{-1}$. Average values of the
453 chemical/structural traits LMA, N_{area} and P_{area} were 110.9×10^3 , 0.19×10^3 and 0.013
454 g m^{-2} with ranges of 12.04 to 610.3×10^3 (LMA), near zero to 1.49g m^{-2} (N_{area}), and
455 near zero to 0.06mg m^{-2} (P_{area}). Average values of χ , H_{max} and WD were 0.71, 26.3 m
456 and 0.55g cm^{-3} with ranges of 0.39 to 0.94, 1.3 to 54.5 m, and 0.33 to 0.98g cm^{-3}
457 respectively.

458 Four orthogonal dimensions of trait variation were identified corresponding to
459 the metabolic, chemical/structural, hydraulic and height trait groups described above
460 (Fig. 2, Table 3). The metabolic traits V_{cmax} , J_{max} and R_{dark} varied continuously and in
461 close correlation with one another. V_{cmax} and χ were negatively correlated, but the
462 correlation was weak (not shown: slope = -1.85 , intercept = 1.32 , $R^2 = 0.13$, $p <$
463 0.05). Table 3 makes it clear that variation in χ in this data set does not belong to the
464 metabolic dimension. The chemical/structural traits LMA, N_{area} and P_{area} were
465 positively correlated with one another ($p < 0.05$), although the pairwise relationship of
466 P_{area} to LMA was weaker than that of N_{area} to LMA. The strong correlation between
467 LMA and N_{area} suggests that much of the N content in the leaves is structural rather
468 than metabolic (see also Yang et al., 2018). A similar result was obtained when mass-
469 rather than area-based nutrient values were used in the PCA (not shown). The third
470 dimension was mostly represented by variation in WD, with some contribution from
471 P_{area} . Finally H_{max} and χ had a non-significant negative pairwise relationship and were
472 associated with the fourth dimension, suggesting a trade-off between water loss and
473 the length of the water-transport pathway. These dimensions of trait variation are
474 broadly in agreement with those described by Baraloto et al. (2010), Fyllas et al.
475 (2012) and Reich (2014).

476 **Contribution of climate variables to trait variation**

477 High and low values for MI, mPAR and MAT were defined as values above or
478 below the mean value of the climate variable. Regression slopes between V_{cmax} and
479 J_{max} for both high MI and low MI groups were close together but statistically distinct
480 ($p < 0.05$, Fig. 3), and the same was true for high *versus* low mPAR and MAT groups
481 (Fig. 3). Regressions for V_{cmax} *versus* N_{area} were not significant within these climatic
482 groups (Fig. 3) but the relationship was significant, albeit weak, when all of the data
483 were considered together (not shown: slope = 0.69 , $R^2 = 0.10$, $p < 0.05$). The

484 weakness of this relationship corroborates our previous assessment of leaf N content
485 as being primarily structural rather than metabolic. High MI and low mPAR were
486 associated with high V_{cmax} , J_{max} , and N_{area} (Fig. 3). These variables were also
487 associated with R_{dark} and LMA. The remaining traits χ , P_{area} , H_{max} and WD were very
488 scattered against MI and mPAR (no significant relationship). All traits had high and
489 low values spanning the full range of MAT.

490 The clustered vectors for metabolic traits, MI and MAT in Fig. 4 indicate that
491 higher moisture and air temperature favour species with higher metabolic rates (Fig.
492 4). The RDA constrained by climate variables explained 35% of trait variation with
493 19% and 11% on axes 1 and 2 respectively ($p < 0.05$, Fig. 4). This represents an
494 unexpectedly large fraction of the trait variation, considering the modest range in
495 MAT (19 to 24°C), mPAR (27.4 to 30.5 mol m⁻²) and MI (0.9 to 2.5; i.e. typical
496 values for non-drought-stressed conditions) among these tropical moist forest sites.
497 No individually significant trait-climate variable relationship was found. An
498 association of high metabolic rates with aridity (Prentice et al., 2011) has been found
499 when considering longer climate gradients, but this is not apparent over the more
500 limited climatic range sampled here.

501 **Contribution of dynamic roles to trait variation**

502 The assignment of the four groups obtained by *K*-means clustering to dynamic
503 roles was based on the degree of correspondence between the mean values of plant
504 traits for each group and the classification by Shugart (1984). H_{max} determined
505 whether a cluster was labeled as climax or large pioneer, or small pioneer or
506 subcanopy. Higher values of photosynthetic traits defined tall trees as climax, as
507 opposed to large pioneer, and small trees as small pioneer, as opposed to subcanopy.

508 Expert (A1) and quantitative (A2) role definitions explained 23% and 55% of
509 total plant trait variance, respectively (Fig. 5). With respect to patterns, the RDA
510 results obtained with the two classifications are quite similar to one another, which is
511 expected as the clustering was performed using the same trait data represented in the
512 RDA. However, the quantitative role definitions explained substantially more
513 variance than the expert definitions. The major common patterns shown in the two
514 RDA plots are as follows:

515

- 516 (1) The metabolic traits V_{cmax} , J_{max} , R_{dark} and the structural-chemical traits N_{area} and
517 LMA tend to be higher in climax species than in the other groups.
518 (2) P_{area} tends to be greater in subcanopy species than in the other groups.
519 (3) WD tends to be smaller in pioneer species than in the other groups.

520

521 These distinctions are supported, and further information provided, by the summary
522 statistics for trait variation within each group (Fig. 6). Climax species consistently
523 have the highest values of V_{cmax} , J_{max} , R_{dark} , LMA and N_{area} . High WD, consistent with
524 slow growth, characterized the subcanopy species. The χ ratio was lowest in climax
525 species and highest in subcanopy species. The scaling slopes of the bivariate
526 relationships between V_{cmax} and J_{max} , and between V_{cmax} and N_{area} , were largely similar
527 within each group, whether the roles were defined quantitatively or by expert
528 assessment (Fig. 7).

529 **Partitioning trait variance to climate variables *versus* dynamic roles**

530 RDA constrained by the two sets of predictors (climate and dynamic roles)
531 both separately and collectively provides the necessary information to partition the
532 total explained variation into the unique contributions of each set and a combined
533 contribution associated with covariation of the two sets, via the Legendre variation
534 partitioning method (Legendre and Anderson, 1999; Peres-Neto et al., 2006; Meng et
535 al., 2015; Yang et al., 2018). Based on the quantitative assessment of dynamic roles
536 (A2), RDA constrained by both sets of predictors explained 61% of trait variation,
537 which could be partitioned as follows: 26% from dynamic roles alone, 6% from
538 climate alone, and 29% from the combination. The corresponding figures based on
539 expert assessment were as follows: 43% of trait variation explained, composed of 8%
540 from dynamic roles alone, 20% from climate alone, and 15% from the combination.

541 Although significant trait variation was linked to climate, individual trait-
542 climate relationships were weak and patterns that have been observed across a wider
543 range of climates, such as the widely reported increase of N_{area} with aridity, were not
544 present. This pattern is to be expected considering that semi-arid and arid ecosystems
545 are not considered. Variance partitioning showed that between 8 and 26% of trait
546 variation (depending on the source of information on dynamics roles) could not be

547 attributed to the temperature and moisture regime, but could be related uniquely to
548 species' dynamic roles.

549 **Unexplained trait variance**

550 Unexplained variance amounted to 57% and 39% for the expert and
551 quantitative assessments, respectively. In principle unexplained variance might be
552 related to a variety of factors including the season of measurement, forest age and
553 aspects of soil fertility. However, dividing the data according to wet-season (*CTR2*,
554 *KBL1*, *KBL3*, *KCR*, *RCRs*) versus dry-season (*CTR1*, *RCRw*, *Y1X*, *Y2U*, *Y3M1*, *Y3M2*,
555 *Y4L*) measurements yielded patterns similar to those found in the full data set. No data
556 on forest age were available. No correlations were found between trait values and soil
557 total N, soil total P and cation exchange capacity (Table 1).

558

559 **Discussion**

560 This study provides support for the idea that forest dynamic roles, as described
561 by Shugart (1984), might be systematically related to the biophysical and
562 ecophysiological traits used in DGVMs. Our analysis explores plant trait diversity and
563 plasticity with a view to more realistic modelling of plant and vegetation processes,
564 whether for local or global model applications (Fyllas et al., 2009; 2012; Quesada et
565 al., 2012). Expert classification of dynamic roles in forests is notoriously difficult
566 because it requires observation over many decades. Our quantitative analyses suggest
567 a possible alternative approach to classification based on trait measurements at one
568 point in time. Moreover, our results have supported certain specific predictions of the
569 least-cost and coordination hypotheses, which are key to explaining species strategies,
570 community assembly and ecosystem structure and function (Reich, 2014). They
571 collectively hold the promise of providing general, testable trait-environment
572 relationships that could reduce the excessive number of parameters required by most
573 DGVMs (Prentice et al., 2015).

574 **Dynamic roles and the coordination hypothesis**

575 Our results support a core prediction of the coordination hypothesis for
576 forests: that J_{\max} and $V_{c\max}$ should be higher under high illumination and lower in the

577 shade, as seen both in the vertical gradient of light-saturated assimilation rates in
578 dense canopies (Chen et al., 1993) and more generally, in the solar radiation gradient
579 across canopies situated in diverse environments (Maire et al., 2012). With respect to
580 dynamic roles, outer-canopy climax species are expected to receive most PAR and
581 therefore should have the highest photosynthetic capacity, while subcanopy species
582 should have the lowest. Pioneer (gap-requiring) species would be expected to have
583 intermediate photosynthetic capacity and this too is consistent with our findings.
584 Additionally, the widely reported conservative ratio of J_{\max} and V_{\max} seems to be
585 maintained, both within and across dynamic roles. The association of R_{dark} with V_{\max}
586 and J_{\max} was also found to be strong, with R_{dark} maintaining a near constant ratio for
587 leaves whether in sun-exposed or shade conditions, as previously reported (e.g. by
588 Hirose and Werger, 1987; Weerasinghe et al., 2014; Atkin et al., 2015).

589 The observed relationships among N_{area} , P_{area} and LMA, and the weaker
590 correlations of these traits with primary metabolic traits, reflect the fact that a
591 substantial part of the N and P content of leaves is not directly tied to photosynthetic
592 functions (Dong et al., 2017). Although strong linear relationships between V_{\max} (at a
593 reference temperature) and N_{area} seem to be widely expected, they are not always
594 found (Prentice et al., 2014; Togashi et al., 2017), perhaps due to the overpowering
595 effect of variation in structural and/or defensive components of leaf N. The
596 photosynthetic component of N_{area} however is expected to be proportional to incident
597 PAR. This expectation is supported by the analysis of Dong et al. (2017), and by our
598 finding of highest N_{area} among climax species.

599 **Dynamic roles and the least-cost hypothesis**

600 It has been reported that χ declines with tree height. This too is a prediction of
601 the least-cost hypothesis (Prentice et al., 2014), as the cost of maintaining the water
602 transport pathway increases at with height. Therefore, tall trees – and the top stratum
603 of leaves in a tall tree, as noted by Koch et al. (2015) – may be expected to aim for a
604 lower optimum χ by investing more in the maintenance of biochemical capacity and
605 less in the maintenance of transport capacity. Even if the path-length effect on stem
606 hydraulic conductance is fully compensated by xylem tapering (Tyree and Ewers,
607 1991; Enquist and Bentley, 2012; Olson et al., 2014) as often seems to be the case, it
608 is still more expensive in terms of sapwood respiration to maintain a tall stem as

609 opposed to a short stem (Prentice et al., 2014). This prediction is supported by the low
610 χ found here in climax species. However, surprisingly, large pioneer species (with
611 H_{\max} equivalent to climax species) did not show this adaptation. Subcanopy species
612 did nonetheless show high χ , consistent with their short stature. Given a reduced χ , the
613 coordination hypothesis then predicts that V_{\max} should be increased. This mechanism
614 may additionally contribute to the high V_{\max} found in climax species and the low
615 V_{\max} in subcanopy species.

616 **Dynamic roles, the leaf economics spectrum and the theory of forest dynamics**

617 A third group of predictions broadly supported by our results comes from the
618 framework presented in Shugart (1984), Turner (2001) and Fyllas et al. (2012). This
619 approach considers two main axes of ecological specialization, one reflecting canopy
620 position and access to light, the other life span and growth rate. The main advantage
621 for large pioneers in rapidly achieving tall stature is to shade lower canopies nearby,
622 while obtaining rapid access to full sunlight. Compared to climax species, large
623 pioneers adopt a less conservative strategy regarding water use, and are likely to have
624 a shorter lifespan (Shugart, 1984; Reich, 2014). One way to achieve fast growth is to
625 invest in low-density conducting tissues, which implies lower WD. Subcanopy
626 species by contrast are necessarily shade-tolerant and often have traits associated with
627 slow growth. Our results support the existence of this tradeoff, with subcanopy trees
628 having generally high WD (a trait often accompanied by a high density of short and
629 narrow vessels: Reich, 2014).

630 According to the LES, across species globally, high LMA is linked to
631 longevity of individual leaves; and it has generally been found that LMA varies as
632 much or more within communities as with environmental gradients (Wright et al.,
633 2004). Our data do not allow us to address the LMA-lifespan linkage directly.
634 However, they do show that LMA varies systematically across the dynamic roles,
635 being greatest in climax species and associated with high V_{\max} and least in subcanopy
636 species where it is associated with low V_{\max} . These findings suggest a more nuanced
637 interpretation of the variation in LMA among dynamic roles. Namely: that thick,
638 high-LMA leaves are a pre-requisite for a leaf to attain V_{\max} commensurate with high
639 levels of PAR at the top of a canopy (Niinemets and Tenhunen, 1997), while thin,
640 low-LMA leaves provide optimum light capture for the least investment in leaves – a

641 good strategy for subcanopy species. Fast-growing pioneer species with their high
642 water-use strategy also require a low investment in leaf structure, developing thin,
643 low-LMA leaves in order to obtain a quicker return on investment (Turner, 2001).
644 The downside is that these leaves are likely to be more exposed to herbivory losses,
645 while the low-density stems are subject to the risks of cavitation and embolism,
646 shortening their life expectancy (Enquist and Bentley, 2012).

647 **Implications for modelling**

648 DGVMs based on continuous trait variation have been developed in response
649 to the growing realization that PFTs, as conventionally defined, do not adequately
650 describe the genotypic or phenotypic plasticity of plant traits in the real world. The
651 existence of systematic, adaptive trait variation in forests, within a climate range
652 where neither moisture nor low temperature is limiting, provides further support for
653 the conclusion (e.g. Meng et al., 2015) that models should not be based on fixed,
654 PFT-specific values for many quantitative traits. In general, consideration of the
655 adaptive function of trait differences among dynamic roles should contribute to
656 reducing the multiplicity of uncertain parameters, and simultaneously increase the
657 realism, of next-generation DGVMs. DGVMs in general (including recent trait-based
658 vegetation models, with the exception of the model of Fyllas et al., 2014 developed
659 for Amazonian forests) have paid minimal attention to the co-existing functional
660 diversity of traits present in communities where climate variation is small but tree
661 species diversity is large, including tropical forests. Our results suggest that the
662 framework provided by optimality concepts (the coordination and least-cost
663 hypotheses) could be combined with classical forest dynamics theory, which
664 differentiates complementary survival strategies for tree species in a highly
665 competitive environment, to yield successful predictions that would allow vegetation
666 dynamics to be represented more faithfully in DGVMs. The combination of these
667 different research strands can be achieved by extending existing predictions about
668 trait-environment relationships based on optimality considerations to cover biotically
669 induced microhabitat variation within complex plant communities.

670 We therefore suggest that the ecophysiological correlates of species dynamical
671 roles be further analysed in other tropical and extratropical forests, as part of the
672 empirical research required to establish a firmer foundation for next-generation

673 vegetation models. Moreover, we look forward to the widespread use of adaptive
674 schemes in which trait combinations, such as those characterizing species' dynamical
675 roles, emerge naturally from the competition among plants.

676

677 **Acknowledgments**

678 This research was funded by the Terrestrial Ecosystem Research Network
679 (TERN, www.tern.org.au), which has been supported by the Australian Government
680 through the National Collaborative Research Infrastructure Strategy (NCRIS), with
681 additional funding provided by Macquarie University and the Australian National
682 University. HFT and ND were supported by Macquarie University International
683 Research Scholarship (iMQRES) awards to ICP. ICP, BJE, HFT and ND have been
684 supported by the Ecosystem Modelling and Scaling Infrastructure Facility (eMAST,
685 <http://www.emast.org.au>). Data were collected in North Queensland at field sites of
686 the Australian SuperSite Network. Both eMAST and the Australian SuperSites
687 Network are facilities of TERN. OA acknowledges the support of the Australian
688 Research Council (DP130101252 and CE140100008). Leaf N and P measurements
689 were made at the Department of Forestry, ANU. We are grateful to Jinlong Zhang
690 (Xishuangbanna Tropical Botanical Garden) for identifying plant species, and also to
691 Jack Egerton (ANU), Li Guangqi (Macquarie), Lingling Zhu (ANU), Danielle Creek
692 (University of Western Sydney), Lucy Hayes (ANU) and Stephanie McCaffery
693 (ANU) for help with fieldwork and/or N and P digestions. We thank Tomas Ferreira
694 Domingues (University of São Paulo) for comments that helped to improve this paper.
695 ND and SPH acknowledge support from the ERC-funded project GC2.0 (Global
696 Change 2.0: Unlocking the past for a clearer future, grant number 694481). This
697 research is a contribution to the AXA Chair Program in Biosphere and Climate
698 Impacts and the Imperial College initiative on Grand Challenges in Ecosystems and
699 the Environment (ICP).

700 **Tables**

701 Table 1. Climate averages (MAT = mean annual temperature, MI = Moisture Index,
 702 mPAR = mean monthly photosynthetic active radiation), geographic location,
 703 elevation above sea level and soil properties (CEC = cation exchange capacity, TN =
 704 total soil nitrogen, TP = total soil phosphorus) of the study sites in north-east
 705 Australia (*CTR1*, *CTR2*, *KBL1*, *KBL3*, *KCR*, *RCRs*, *RCRw*) and south-east China
 706 (*Y1X*, *Y2U*, *Y3M1*, *Y3M2*, *Y4L*).

SITE	LON	LAT	Altitude (m)	MAT (°C)	MAP (mm)	mPAR (mol/m ²)	MI	CEC(cmol/kg)	TN (%)	TP (%)
CTR1	145.45	-16.10	64	24.4	5143	27.5	2.54	11.8	0.64	0.023
CTR2	145.45	-16.10	90	24.4	5143	27.5	2.54	11.8	0.02	0.011
KBL1	145.54	-17.76	761	20.4	1976	28.2	1.39	10.83	0.08	0.030
KBL3	145.54	-17.69	1055	19.0	1726	28.3	1.22	11.11	0.08	0.030
KCR	145.60	-17.11	813	19.6	2541	27.9	1.82	9.81	0.01	0.006
RCRs	145.63	-17.12	700	19.4	2246	27.9	1.29	4.3	0.18	0.019
RCRw	145.63	-17.12	700	19.4	2246	27.9	1.29	4.3	0.18	0.019
Y1X	101.27	21.92	502	21.7	1427	30.1	0.94	8.68	0.08	0.044
Y2U	101.24	21.98	1075	19.7	1562	30.6	1.03	6.09	0.08	0.044
Y3M1	101.58	21.61	668	19.6	1662	29.8	1.14	10.21	0.08	0.050
Y3M2	101.58	21.62	828	20.5	1604	29.9	1.07	10.21	0.08	0.050
Y4L	101.58	21.62	1034	20.5	1604	30.1	1.06	10.21	0.08	0.050

707

708 Table 2. Geographic distribution of expert assessment of dynamic roles per number of
 709 species and per number of leaves for the study sites in north-east Australia (*CTR1*,
 710 *CTR2*, *KBL1*, *KBL3*, *KCR*, *RCRs*, *RCRw*) and south-east China (*Y1X*, *Y2U*, *Y3M1*,
 711 *Y3M2*, *Y4L*). This dataset includes 262 observations.

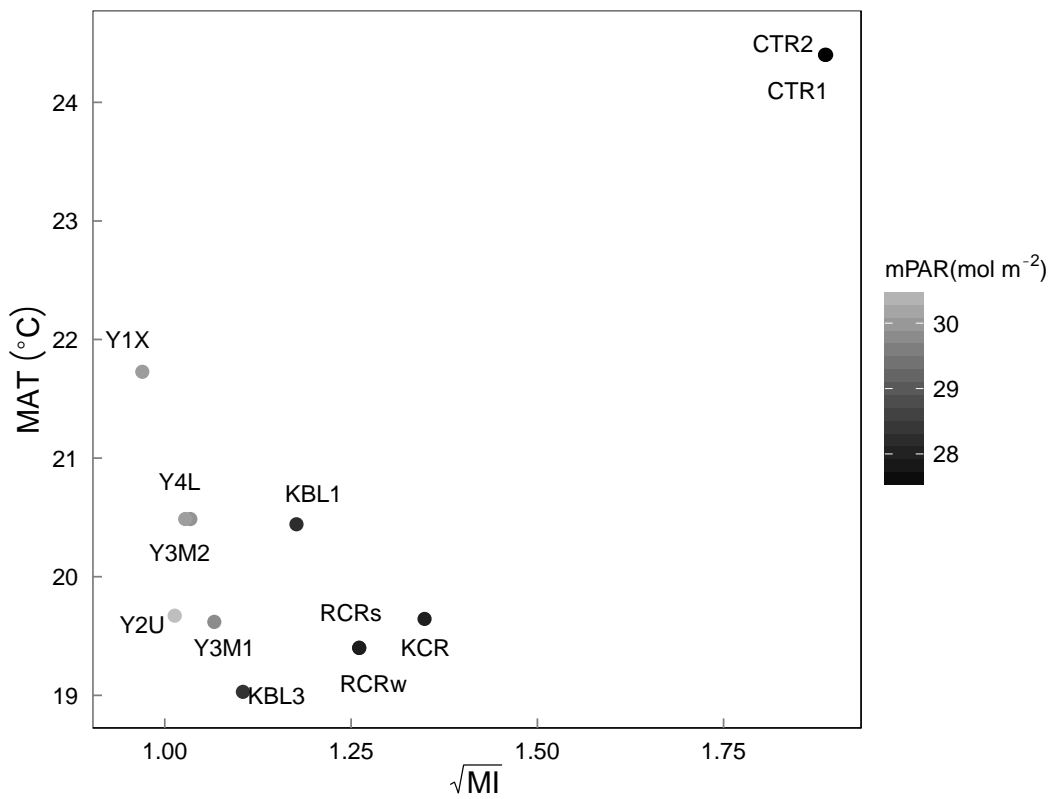
SITE	Number of species				Number of leaves			
	climax	large pioneer	Small pioneer	subcanopy	climax	large pioneer	Small pioneer	subcanopy
CTR1	7	4		1	27	16		4
CTR2	4	1			11	5		
KBL1	2	4			7	25		
KBL3	3	4			17	13		
KCR	3	5			9	17		
RCRs	7	16	3	4	9	52	7	4
RCRw		8	1			26	4	
Y1X		2				2		
Y2U		3		1		3		1
Y3M1				1				2
Y3M2				1				1
Y4L								

712

713 Table 3. Principal Component Analysis loadings for nine traits. The highest
 714 correlations (absolute magnitudes > 0.45) are indicated in bold.

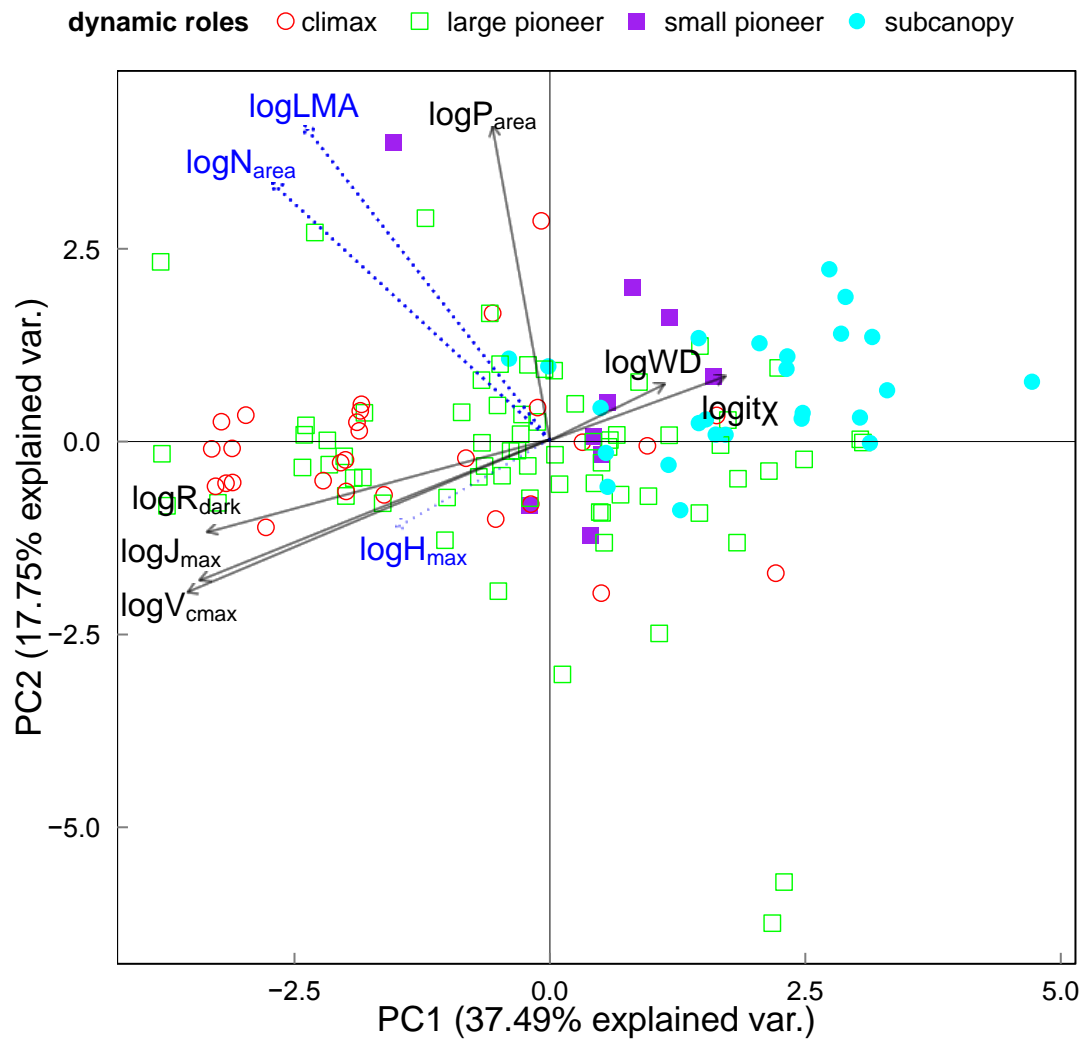
	PC1	PC2	PC3	PC4
log V _{cmax}	-0.48	-0.27	0.21	0
log J _{max}	-0.46	-0.25	0.18	0.04
log R _{dark}	-0.45	-0.16	0.27	-0.01
log LMA	-0.32	0.55	-0.21	0.03
log N _{area}	-0.37	0.45	-0.24	-0.12
log P _{area}	-0.08	0.54	0.45	0.03
log WD	0.15	0.1	0.68	-0.16
log H _{max}	-0.2	-0.15	-0.24	-0.74
logit χ	0.23	0.11	0.16	-0.64
	PC1	PC2	PC3	PC4
Standard deviation	1.84	1.26	1.09	0.98
Proportion of Variance	0.37	0.18	0.13	0.11
Cumulative Proportion	0.37	0.55	0.68	0.79

715



717

718 Fig. 1. Mean annual temperature (MAT, °C), the square root of Moisture Index (MI,
 719 ratio of precipitation to equilibrium evapotranspiration) and mean monthly
 720 photosynthetic active radiation (mPAR, mol m⁻²) for northern Australia (*CTR1*,
 721 *CTR2*, *KBL1*, *KBL3*, *KCR*, *RCRs*, *RCRw*) and southwestern China (*Y1X*, *Y2U*, *Y3M1*,
 722 *Y3M2*, *Y4L*).



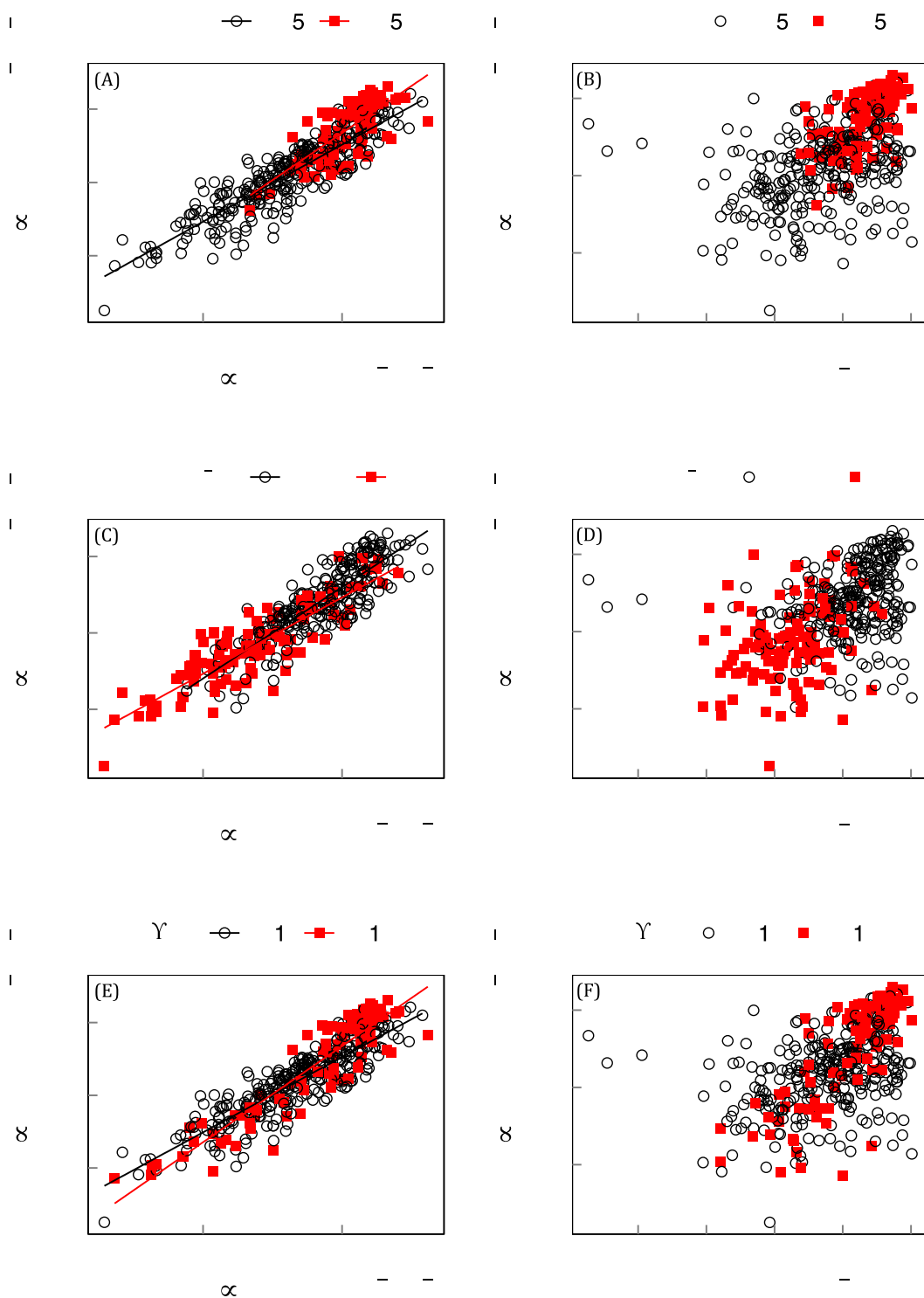
723

724 Fig. 2. Principal component analysis (PCA) of nine traits in northern Australia and

725 southwestern China ($n = 130$). Blue dotted lines and names extend backwards from

726 the plane of the paper; and black lines and names protrude forwards towards the

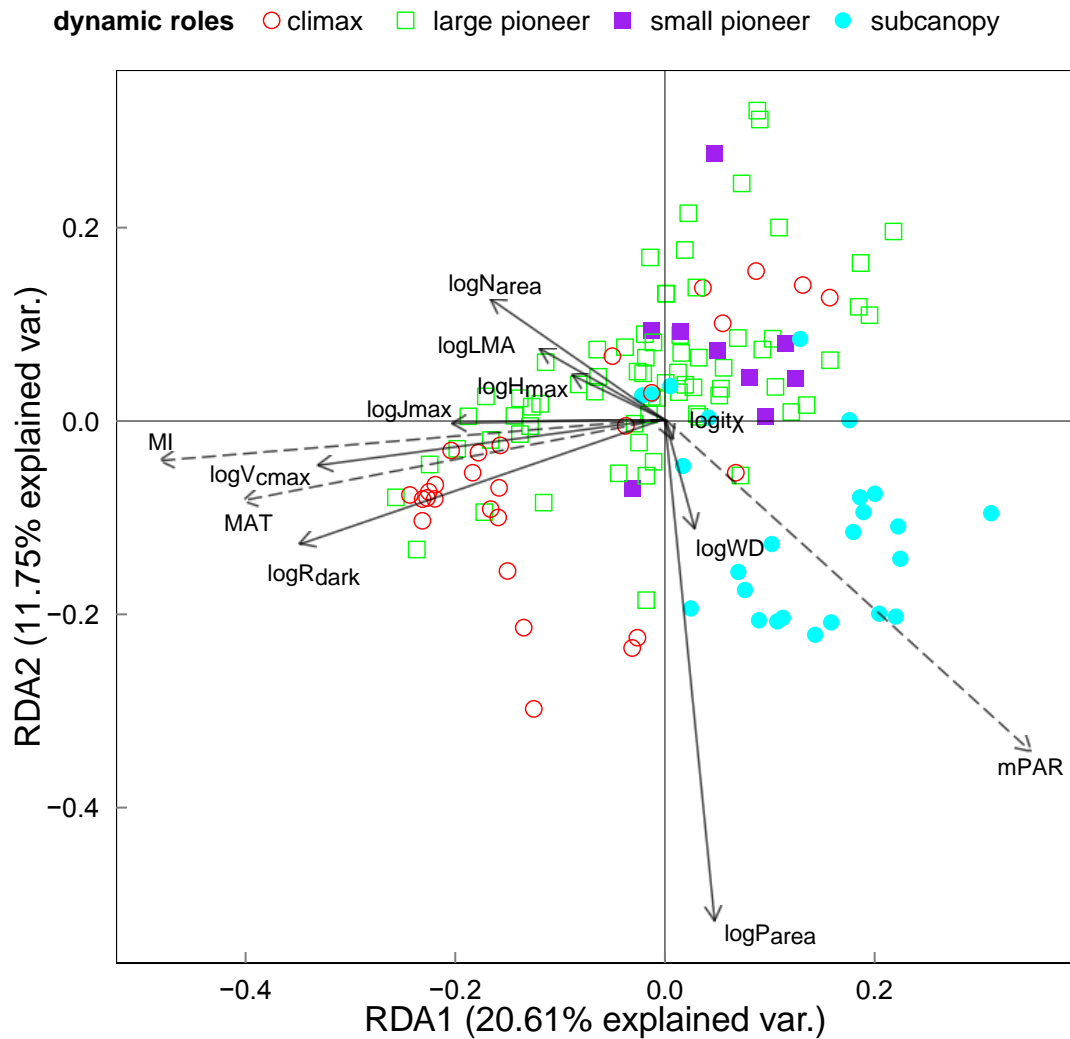
727 observer.



728

729 Fig. 3. Bivariate relationships of $\log_{10}V_{cmax}$ versus $\log_{10}J_{max}$ and $\log_{10}V_{cmax}$ versus
 730 $\log_{10}N_{area}$, within groups defined by high and low values of climate variables (3A and
 731 3B: MI; 3C and 3D: mPAR; 3E and 3F: MAT) (n = 431). Only significant linear
 732 regressions ($p < 0.05$) are shown.

733

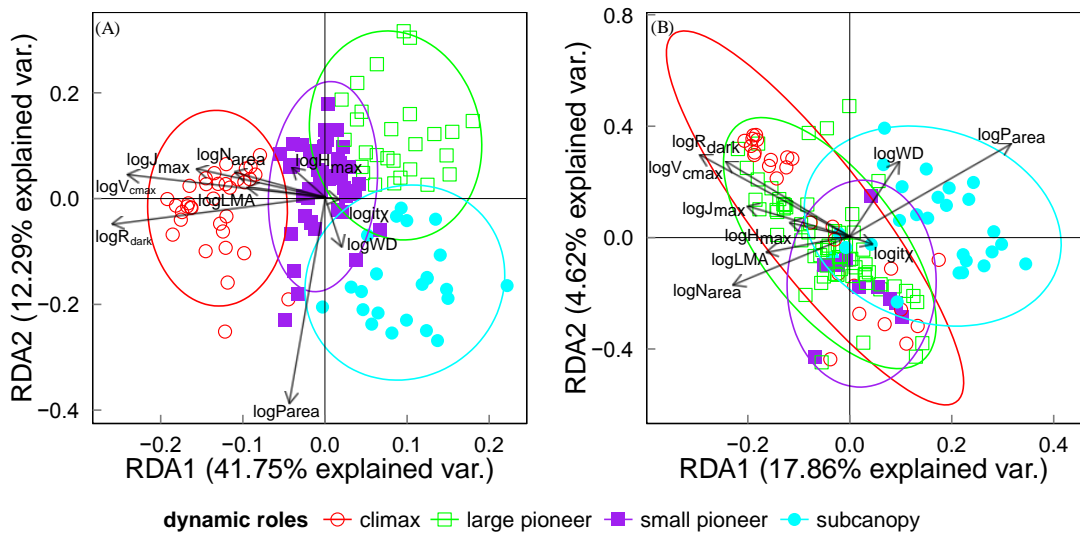


735

736 Fig. 4. Redundancy analysis (RDA) of nine traits constrained by climate variables
 737 Mean annual temperature (MAT, °C), the square root of Moisture Index (MI, ratio of
 738 precipitation to equilibrium evapotranspiration) and mean monthly photosynthetic
 739 active radiation (mPAR, mol m⁻²) ($n = 130$, $p < 0.05$). Dynamic roles do not
 740 participate in this RDA calculation and are shown for visual comparison only.

741

742



743

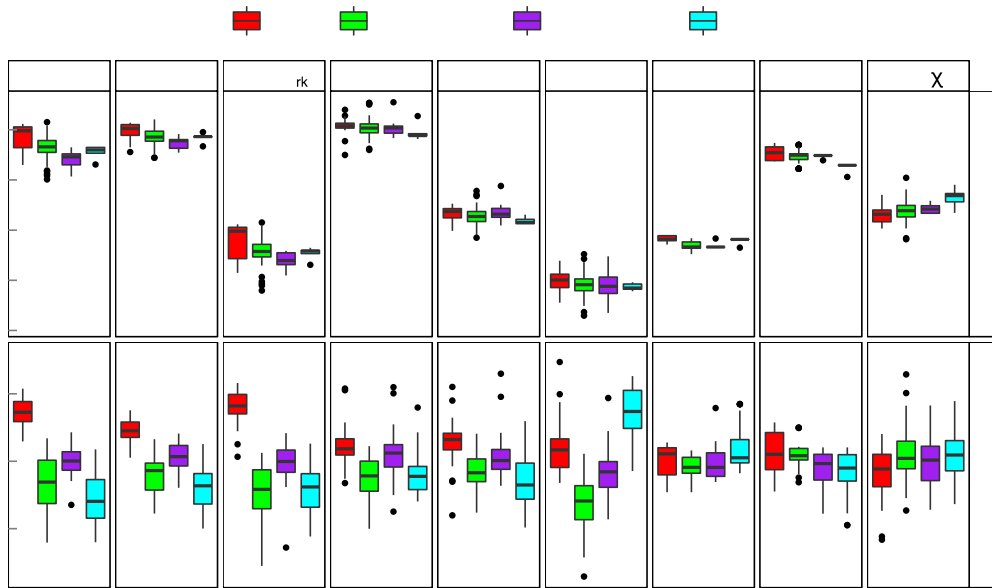
744

745

746

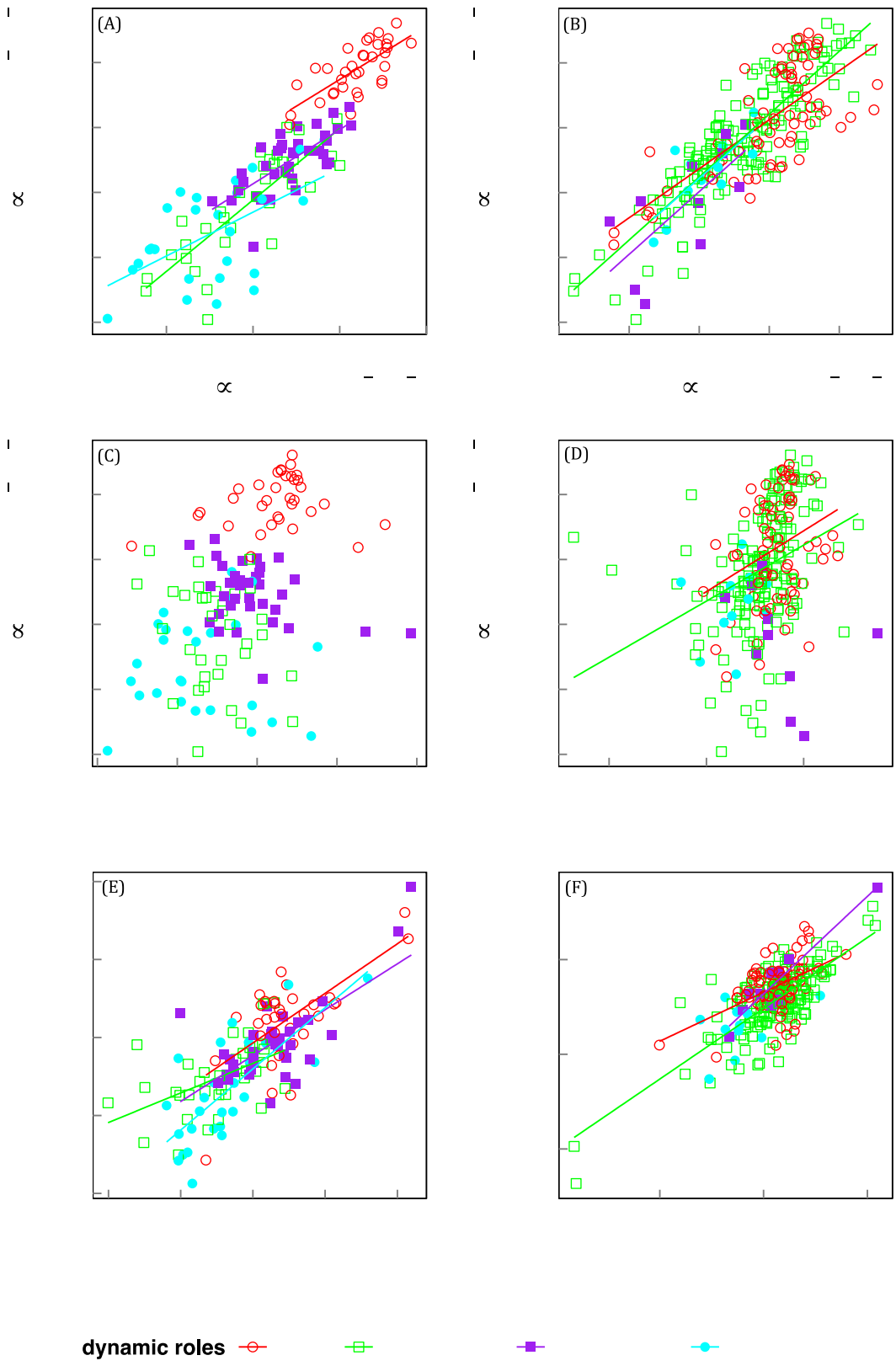
747

Fig. 5. Redundancy analysis (RDA) of nine traits constrained by dynamic roles, defined by quantitative (5A) *versus* expert (5B) assessment ($n = 130$). Ellipses represent 95% confidence intervals around the centroid of each group.



749

750 Fig. 6. Box plots showing means and standard deviation of nine traits according to the
 751 four dynamic roles based on quantitative *versus* expert assessment ($n = 130$, $p <$
 752 0.05). ‘Expert’ group averages of LMA, N_{area} and P_{area} are not significantly different
 753 (ANOVA). Dynamic roles of each trait sharing the same letter (Tukey *post hoc* test)
 754 are not significantly different.



755

756 Fig. 7. Bivariate relationships of V_{cmax} versus J_{max} , V_{cmax} versus N_{area} (upper panels)

757 and N_{area} versus LMA (lower panels) within dynamic role groups, according to

758 quantitative (left, $n = 130$) *versus* expert (right, $n = 262$) assessment. Significant linear
759 regressions between \log_{10} -transformed variables are shown ($p < 0.05$).
760

761 **References**

- 762 Allen, S.E., Grimshaw, H., Parkinson, J.A., Quarmby, C., 1974. Chemical analysis of
763 ecological materials. Blackwell Scientific Publications.
- 764 Atkin, O.K., Bloomfield, K.J., Reich, P.B., Tjoelker, M.G., Asner, G.P., Bonal, D.,
765 Bönisch, G., Bradford, M.G., Cernusak, L.A., Cosio, E.G., Creek, D., Crous, K.Y.,
766 Domingues, T.F., Dukes, J.S., Egerton, J.J.G., Evans, J.R., Farquhar, G.D., Fyllas, N.M.,
767 Gauthier, P.P.G., Gloor, E., Gimeno, T.E., Griffin, K.L., Guerrieri, R., Heskell, M.A.,
768 Huntingford, C., Ishida, F.Y., Kattge, J., Lambers, H., Liddell, M.J., Lloyd, J., Lusk,
769 C.H., Martin, R.E., Maksimov, A.P., Maximov, T.C., Malhi, Y., Medlyn, B.E., Meir, P.,
770 Mercado, L.M., Mirotchnick, N., Ng, D., Niinemets, Ü., O'Sullivan, O.S., Phillips, O.L.,
771 Poorter, L., Poot, P., Prentice, I.C., Salinas, N., Rowland, L.M., Ryan, M.G., Sitch, S.,
772 Slot, M., Smith, N.G., Turnbull, M.H., VanderWel, M.C., Valladares, F., Veneklaas,
773 E.J., Weerasinghe, L.K., Wirth, C., Wright, I.J., Wythers, K.R., Xiang, J., Xiang, S.,
774 Zaragoza-Castells, J., 2015. Global variability in leaf respiration in relation to
775 climate, plant functional types and leaf traits. *New Phytologist* 206, 614–636.
- 776 Atkin, O.K., Holly, C., Ball, M.C., 2000. Acclimation of snow gum (*Eucalyptus*
777 *pauciflora*) leaf respiration to seasonal and diurnal variations in temperature:
778 the importance of changes in the capacity and temperature sensitivity of
779 respiration. *Plant, Cell & Environment* 23, 15-26.
- 780 Baraloto, C., Timothy Paine, C., Poorter, L., Beauchene, J., Bonal, D., Domenach,
781 A.M., Hérault, B., Patino, S., Roggy, J.C., Chave, J., 2010. Decoupled leaf and stem
782 economics in rain forest trees. *Ecology Letters* 13, 1338-1347.
- 783 Bernacchi, C.J., Pimentel, C., Long, S.P., 2003. In vivo temperature response
784 functions of parameters required to model RuBP-limited photosynthesis. *Plant,*
785 *Cell & Environment* 26, 1419-1430.
- 786 Bernacchi, C.J., Singsaas, E.L., Pimentel, C., Portis Jr, A.R., Long, S.P., 2001.
787 Improved temperature response functions for models of Rubisco-limited
788 photosynthesis. *Plant, Cell & Environment* 24, 253-259.
- 789 Bloomfield, K.J., Domingues, T.F., Saiz, G., Bird, M.I., Crayn, D.M., Ford, A., Metcalfe,
790 D.J., Farquhar, G.D., Lloyd, J., 2014. Contrasting photosynthetic characteristics of
791 forest vs. savanna species (far North Queensland, Australia). *Biogeosciences* 11,
792 7331-7347, <https://doi.org/7310.5194/bg-7311-7331-2014>.
- 793 Botkin, D.B., Janak, J.F., Wallis, J.R., 1972. Some ecological consequences of a
794 computer model of forest growth. *The Journal of Ecology*, 849-872.
- 795 Box, E.O., 1981. Predicting physiognomic vegetation types with climate variables.
796 *Vegetatio* 45, 127-139.
- 797 Bradford, M.G., Metcalfe, D.J., Ford, A., Liddell, M.J., McKeown, A., 2014a.
798 Floristics, stand structure and aboveground biomass of a 25-ha rainforest plot in
799 the wet tropics of Australia. *Journal of Tropical Forest Science* 26, 543-553.
- 800 Bradford, M.G., Murphy, H.T., Ford, A.J., Hogan, D.L., Metcalfe, D.J., 2014b. Long-
801 term stem inventory data from tropical rain forest plots in Australia. *Ecology* 95,
802 2362-2000.
- 803 Calvin, M., Benson, A.A., 1948. The path of carbon in photosynthesis. US Atomic
804 Energy Commission, Technical Information Division.
- 805 Chen, J.-L., Reynolds, J., Harley, P., Tenhunen, J., 1993. Coordination theory of leaf
806 nitrogen distribution in a canopy. *Oecologia* 93, 63-69.
- 807 De Kauwe, M.G., Lin, Y.-S., Wright, I.J., Medlyn, B.E., Crous, K.Y., Ellsworth, D.S.,
808 Maire, V., Prentice, I.C., Atkin, O.K., Rogers, A., Niinemets, Ü., Serbin, S.P., Meir, P.,
809 Uddling, J., Togashi, H.F., Tarvainen, L., Weerasinghe, L.K., Evans, B.J., Ishida, F.Y.,

810 Domingues, T.F., 2016. A test of the 'one-point method' for estimating maximum
811 carboxylation capacity from field-measured, light-saturated photosynthesis. *New*
812 *Phytologist* 210, 1130-1144.

813 Denslow, J.S., 1987. Tropical rainforest gaps and tree species diversity. *Annual*
814 *Review of Ecology and Systematics* 18, 431-451.

815 Dewar, R., Mauranen, A., Mäkelä, A., Hölttä, T., Medlyn, B., Vesala, T., 2018. New
816 insights into the covariation of stomatal, mesophyll and hydraulic conductances
817 from optimization models incorporating nonstomatal limitations to
818 photosynthesis. *New Phytologist* 217, 571-585.

819 Díaz, S., Cabido, M., 1997. Plant functional types and ecosystem function in
820 relation to global change. *Journal of Vegetation Science* 8, 463-474.

821 Domingues, T.F., Meir, P., Feldpausch, T.R., Saiz, G., Veenendaal, E.M., Schrodte, F.,
822 Bird, M., Djangbletey, G., Hien, F., Compaore, H., Diallo, A., Grace, J., Lloyd, J.O.N.,
823 2010. Co-limitation of photosynthetic capacity by nitrogen and phosphorus in
824 West Africa woodlands. *Plant, Cell & Environment* 33, 959-980.

825 Dong, N., Prentice, I.C., Evans, B.J., Caddy-Retalic, S., Lowe, A.J., Wright, I.J., 2017.
826 Leaf nitrogen from first principles: field evidence for adaptive variation with
827 climate. *Biogeosciences* 14, 481-495.

828 Enquist, B.J., Bentley, L.P., 2012. Land plants: new theoretical directions and
829 empirical prospects. *Metabolic Ecology: A Scaling Approach*. Hoboken, NJ: Wiley-
830 Blackwell, 164-187.

831 Evans, J., 1989. Photosynthesis and nitrogen relationships in leaves of C₃ plants.
832 *Oecologia* 78, 9-19.

833 Farquhar, G.D., von Caemmerer, S., Berry, J.A., 1980. A biochemical model of
834 photosynthetic CO₂ assimilation in leaves of C₃ species. *Planta* 149, 78-90.

835 Fisher, R., Muszala, S., Verteinstein, M., Lawrence, P., Xu, C., McDowell, N., Knox,
836 R., Koven, C., Holm, J., Rogers, B., 2015. Taking off the training wheels: the
837 properties of a dynamic vegetation model without climate envelopes,
838 CLM4.5(ED) Geoscientific Model Development 8, 3593-3619.

839 Friend, A., Schugart, H., Running, S., 1993. A physiology-based gap model of
840 forest dynamics. *Ecology* 74, 792-797.

841 Fyllas, N., Gloor, E., Mercado, L., Sitch, S., Quesada, C., Domingues, T., Galbraith, D.,
842 Torre-Lezama, A., Vilanova, E., Ramírez-Angulo, H., 2014. Analysing Amazonian
843 forest productivity using a new individual and trait-based model (TFS v. 1).
844 *Geoscientific Model Development* 7, 1251-1269.

845 Fyllas, N.M., Patino, S., Baker, T., Bielefeld Nardoto, G., Martinelli, L., Quesada, C.,
846 Paiva, R., Schwarz, M., Horna, V., Mercado, L., 2009. Basin-wide variations in
847 foliar properties of Amazonian forest: phylogeny, soils and climate.
848 *Biogeosciences* 6, 2677-2708.

849 Fyllas, N.M., Quesada, C.A., Lloyd, J., 2012. Deriving Plant Functional Types for
850 Amazonian forests for use in vegetation dynamics models. *Perspectives in Plant*
851 *Ecology, Evolution and Systematics* 14, 97-110.

852 Hancock, P., Hutchinson, M., 2006. Spatial interpolation of large climate data sets
853 using bivariate thin plate smoothing splines. *Environmental Modelling &*
854 *Software* 21, 1684-1694.

855 Harris, I., Jones, P.D., Osborn, T.J., Lister, D.H., 2014. Updated high-resolution
856 grids of monthly climatic observations – the CRU TS3.10 Dataset. *International*
857 *Journal of Climatology* 34, 623-642.

858 Harrison, S.P., Prentice, I.C., Barboni, D., Kohfeld, K.E., Ni, J., Sutra, J.P., 2010.
859 Ecophysiological and bioclimatic foundations for a global plant functional
860 classification. *Journal of Vegetation Science* 21, 300-317.
861 Haxeltine, A., Prentice, I.C., 1996. A General Model for the Light-Use Efficiency of
862 Primary Production. *Functional Ecology* 10, 551-561.
863 Hirose, T., Werger, M.J., 1987. Nitrogen use efficiency in instantaneous and daily
864 photosynthesis of leaves in the canopy of a *Solidago altissima* stand. *Physiologia*
865 *Plantarum* 70, 215-222.
866 Hutchinson, M., 2014a. Daily maximum precipitation: ANUClimate 1.0, 0.01
867 degree, Australian Coverage, 1970-2012.
868 Hutchinson, M., 2014b. Daily minimum temperature: ANUClimate 1.0, 0.01
869 degree, Australian Coverage, 1970-2012.
870 Hutchinson, M., 2014c. Daily precipitation: ANUClimate 1.0, 0.01 degree,
871 Australian Coverage, 1970-2012.
872 Koch, G.W., Sillett, S.C., Antoine, M.E., Williams, C.B., 2015. Growth maximization
873 trumps maintenance of leaf conductance in the tallest angiosperm. *Oecologia*
874 177, 321-331.
875 Köppen, W.P., 1931. *Grundriss der klimakunde*. Walter de Gruyter Berlin.
876 Kortschak, H.P., Hartt, C.E., Burr, G.O., 1965. Carbon dioxide fixation in sugarcane
877 leaves. *Plant Physiology* 40, 209.
878 Langan, L., Higgins, S. I. and Scheiter, S., 2017. Climate - biomes, pedo - biomes
879 or pyro - biomes: which world view explains the tropical forest - savanna
880 boundary in South America? *Journal of Biogeography*, 44: 2319-2330.
881 Lavorel, S., Garnier, E., 2002. Predicting changes in community composition and
882 ecosystem functioning from plant traits: revisiting the Holy Grail. *Functional*
883 *Ecology* 16, 545-556.
884 Legendre, P., Anderson, M.J., 1999. Distance - based redundancy analysis: testing
885 multispecies responses in multifactorial ecological experiments. *Ecological*
886 *Monographs* 69, 1-24.
887 Li, G., Harrison, S.P., Prentice, I.C., Falster, D., 2014. Simulation of tree-ring widths
888 with a model for primary production, carbon allocation, and growth.
889 *Biogeosciences* 11, 6711-6724.
890 Liddell, M., 2013a. Cape Tribulation OzFlux tower site OzFlux: Australian and
891 New Zealand Flux Research and Monitoring TERN hdl: 102.100.100/14242.
892 Liddell, M., 2013b. Robson Creek OzFlux tower site OzFlux: Australian and New
893 Zealand Flux Research and Monitoring. TERN hdl: 102.100.100/14243.
894 Lin, Y.-S., Medlyn, B.E., De Kauwe, M.G., Ellsworth, D.S., 2013. Biochemical
895 photosynthetic responses to temperature: how do interspecific differences
896 compare with seasonal shifts? *Tree Physiology* 33, 793-806.
897 Lin, Y.-S., Medlyn, B.E., Duursma, R.A., Prentice, I.C., Wang, H., Baig, S., Eamus, D.,
898 de Dios, V.R., Mitchell, P., Ellsworth, D.S., de Beeck, M.O., Wallin, G., Uddling, J.,
899 Tarvainen, L., Linderson, M.-L., Cernusak, L.A., Nippert, J.B., Ocheltree, T.W.,
900 Tissue, D.T., Martin-StPaul, N.K., Rogers, A., Warren, J.M., De Angelis, P., Hikosaka,
901 K., Han, Q., Onoda, Y., Gimeno, T.E., Barton, C.V.M., Bennie, J., Bonal, D., Bosc, A.,
902 Low, M., Macinins-Ng, C., Rey, A., Rowland, L., Setterfield, S.A., Tausz-Posch, S.,
903 Zaragoza-Castells, J., Broadmeadow, M.S.J., Drake, J.E., Freeman, M., Ghannoum,
904 O., Hutley, L.B., Kelly, J.W., Kikuzawa, K., Kolari, P., Koyama, K., Limousin, J.-M.,
905 Meir, P., Lola da Costa, A.C., Mikkelsen, T.N., Salinas, N., Sun, W., Wingate, L., 2015.

906 Optimal stomatal behaviour around the world. *Nature Climate Change* 5, 459-
907 464.

908 Lloyd, J., Bloomfield, K., Domingues, T.F., Farquhar, G.D., 2013. Photosynthetically
909 relevant foliar traits correlating better on a mass vs an area basis: of
910 ecophysiological relevance or just a case of mathematical imperatives and
911 statistical quicksand? *New Phytologist* 199, 311-321.

912 Lombardozzi, D.L., Smith, N.G., Cheng, S.J., Dukes, J.S., Sharkey, T.D., Rogers, A.,
913 Fisher, R. and Bonan, G.B., 2018. Triose phosphate limitation in photosynthesis
914 models reduces leaf photosynthesis and global terrestrial carbon storage.
915 *Environmental Research Letters* 13(7), 074025.

916 Maire, V., Martre, P., Kattge, J., Gastal, F., Esser, G., Fontaine, S., Soussana, J.-F.,
917 2012. The coordination of leaf photosynthesis links C and N fluxes in C₃ plant
918 species. *PLoS ONE* 7, e38345.

919 Medlyn, B.E., Duursma, R.A., Eamus, D., Ellsworth, D.S., Prentice, I.C., Barton,
920 C.V.M., Crous, K.Y., De Angelis, P., Freeman, M., Wingate, L., 2011. Reconciling the
921 optimal and empirical approaches to modelling stomatal conductance. *Global*
922 *Change Biology* 17, 2134-2144.

923 Medvigy, D., Wofsy, S.C., Munger, J.W., Hollinger, D.Y., Moorcroft, P.R., 2009.
924 Mechanistic scaling of ecosystem function and dynamics in space and time:
925 Ecosystem Demography model version 2. *Journal of Geophysical Research:*
926 *Biogeosciences* 114, 0148-0227.

927 Meng, T., Wang, H., Harrison, S., Prentice, I., Ni, J., Wang, G., 2015. Responses of
928 leaf traits to climatic gradients: adaptive variation versus competition shifts.
929 *Biogeosciences* 12, 5339-5352.

930 Miyazawa, Y., Kikuzawa, K., 2006. Physiological basis of seasonal trend in leaf
931 photosynthesis of five evergreen broad-leaved species in a temperate deciduous
932 forest. *Tree Physiology* 26, 249-256.

933 Moorcroft, P.R., Hurtt, G.C., Pacala, S.W., 2001. A method for scaling vegetation
934 dynamics: The Ecosystem Demography Model (ED). *Ecological Monographs* 71,
935 557-586.

936 Niinemets, Ü., Tenhunen, J.D., 1997. A model separating leaf structural and
937 physiological effects on carbon gain along light gradients for the shade-tolerant
938 species *Acer saccharum*. *Plant, Cell & Environment* 20, 845-866.

939 Oksanen, J., Blanchet, F.G., Kindt, R., Legendre, P., Minchin, P.R., O'Hara, R.,
940 Simpson, G.L., Solymos, P., Stevens, M.H.H., Wagner, H., 2015. Package 'vegan'.
941 *Community ecology package, version, 2.2-1*.

942 Olson, M.E., Anfodillo, T., Rosell, J.A., Petit, G., Crivellaro, A., Isnard, S., León -
943 Gómez, C., Alvarado - Cárdenas, L.O., Castorena, M., 2014. Universal hydraulics of
944 the flowering plants: vessel diameter scales with stem length across angiosperm
945 lineages, habits and climates. *Ecology Letters* 17, 988-997.

946 Pavlick, R., Drewry, D.T., Bohn, K., Reu, B., Kleidon, A., 2013. The Jena Diversity-
947 Dynamic Global Vegetation Model (JeDi-DGVM): a diverse approach to
948 representing terrestrial biogeography and biogeochemistry based on plant
949 functional trade-offs. *Biogeosciences* 10, 4137-4177.

950 Peres-Neto, P.R., Legendre, P., Dray, S., Borcard, D., 2006. Variation partitioning
951 of species data matrices: estimation and comparison of fractions. *Ecology* 87,
952 2614-2625.

953 Prentice, I., Leemans, R., 1990. Pattern and process and the dynamics of forest
954 structure: a simulation approach. *The Journal of Ecology*, 340-355.

955 Prentice, I.C., Bondeau, A., Cramer, W., Harrison, S.P., Hickler, T., Lucht, W., Sitch,
956 S., Smith, B., Sykes, M.T., 2007. Dynamic global vegetation modeling: quantifying
957 terrestrial ecosystem responses to large-scale environmental change, *Terrestrial*
958 *ecosystems in a changing world*. In: Canadell J.G., Pataki D.E., Pitelka L.F. (eds)
959 *Terrestrial Ecosystems in a Changing World*. Global Change — The IGBP Series.
960 Springer, Berlin, Heidelberg, pp. 175-192.

961 Prentice, I.C., Cowling, S.A., 2013. Dynamic global vegetation models, in: Levin,
962 S.A., Academic Press (Ed.), *Encyclopedia of Biodiversity*, 2nd edition ed, pp. 607-
963 689.

964 Prentice, I.C., Cramer, W., Harrison, S.P., Leemans, R., Monserud, R.A., Solomon,
965 A.M., 1992. A global biome model based on plant physiology and dominance, soil
966 properties and climate. *Journal of Biogeography* 19, 117-134.

967 Prentice, I.C., Dong, N., Gleason, S.M., Maire, V., Wright, I.J., 2014. Balancing the
968 costs of carbon gain and water transport: testing a new theoretical framework
969 for plant functional ecology. *Ecology Letters* 17, 82-91.

970 Prentice, I.C., Liang, X., Medlyn, B.E., Wang, Y.P., 2015. Reliable, robust and
971 realistic: the three R's of next-generation land-surface modelling. *Atmospheric*
972 *Chemistry and Physics* 15, 5987-6005.

973 Prentice, I.C., Liddell, M., Furstenau Togashi, H., Atkin, O., Weerasinghe, L., 2013.
974 Leaf Level Physiology, Chemistry and Structural Traits, Far North Queensland
975 SuperSite, Robson Creek, 2012. TERN Australian SuperSite Network.
976 <http://portal.tern.org.au/leaf-level-physiology-creek-2012> 12.

977 Prentice, I.C., Meng, T., Wang, H., Harrison, S.P., Ni, J., Wang, G., 2011. Evidence of
978 a universal scaling relationship for leaf CO₂ drawdown along an aridity gradient.
979 *New Phytologist* 190, 169-180.

980 Prentice, I.C., Sykes, M.T., Cramer, W., 1993. A simulation model for the transient
981 effects of climate change on forest landscapes. *Ecological Modelling* 65, 51-70.

982 Purves, D.W., Lichstein, J.W., Strigul, N., Pacala, S.W., 2008. Predicting and
983 understanding forest dynamics using a simple tractable model. *Proceedings of*
984 *the National Academy of Sciences* 105, 17018.

985 Quesada, C.A., Phillips, O.L., Schwarz, M., Czimczik, C.I., Baker, T.R., Patino, S.,
986 Fyllas, N.M., Hodnett, M.G., Herrera, R., Almeida, S., Alvarez Dávila, E., Arneith, A.,
987 Arroyo, L., Chao, K. J., Dezzeo, N., Erwin, T., di Fiore, A., Higuchi, N., Honorio
988 Coronado, E., Jimenez, E. M., Killeen, T., Lezama, A. T., Lloyd, G., López-González,
989 G., Luizão, F. J., Malhi, Y., Monteagudo, A., Neill, D. A., Núñez Vargas, P., Paiva, R.,
990 Peacock, J., Peñuela, M. C., Peña Cruz, A., Pitman, N., Priante Filho, N., Prieto, A.,
991 Ramírez, H., Rudas, A., Salomão, R., Santos, A. J. B., Schmerler, J., Silva, N., Silveira,
992 M., Vásquez, R., Vieira, I., Terborgh, J., and Lloyd, J., 2012. Basin-wide variations
993 in Amazon forest structure and function are mediated by both soils and climate.
994 *Biogeosciences* 9, 2203-2246.

995 R Core Team, 2012. R: A language and environment for statistical computing. R
996 Foundation for Statistical Computing, Vienna, Austria. [http://www.R-](http://www.R-project.org/)
997 [project.org/](http://www.R-project.org/).

998 Ranson, S.L., Thomas, M., 1960. Crassulacean Acid Metabolism. *Annual Review of*
999 *Plant Physiology* 11, 81-110.

1000 Raunkiaer, C., 1934. *The Life Forms of Plants and Statistical Plant Geography*.
1001 Clarendon Press.

1002 Reich, P.B., 2014. The world-wide 'fast-slow' plant economics spectrum: a traits
1003 manifesto. *Journal of Ecology* 102, 275-301.

1004 Reich, P.B., Walters, M.B., Ellsworth, D.S., 1997. From tropics to tundra: global
1005 convergence in plant functioning. *Proceedings of the National Academy of*
1006 *Sciences* 94, 13730-13734.

1007 Reid, D.E.B., Silins, U., Mendoza, C., Lieffers, V.J., 2005. A unified nomenclature for
1008 quantification and description of water conducting properties of sapwood xylem
1009 based on Darcy's law. *Tree Physiology* 25, 993-1000.

1010 Sakschewski, B., Bloh, W., Boit, A., Rammig, A., Kattge, J., Poorter, L., Peñuelas, J.,
1011 Thonicke, K., 2015. Leaf and stem economics spectra drive diversity of functional
1012 plant traits in a dynamic global vegetation model. *Global Change Biology* 21,
1013 2711-2725.

1014 Scheiter, S., Langan, L., Higgins, S.I., 2013. Next - generation dynamic global
1015 vegetation models: learning from community ecology. *New Phytologist* 198, 957-
1016 969.

1017 Sharkey, T.D., Bernacchi, C.J., Farquhar, G.D., Singsaas, E.L., 2007. Fitting
1018 photosynthetic carbon dioxide response curves for C₃ leaves. *Plant, Cell &*
1019 *Environment* 30, 1035-1040.

1020 Shugart, H.H., 1984. *A Theory of Forest Dynamics*. Springer-Verlag, New York.

1021 Sitch, S., Smith, B., Prentice, I.C., Arneth, A., Bondeau, A., Cramer, W., Kaplan, J.O.,
1022 Levis, S., Lucht, W., Sykes, M.T., Thonicke, K., Venevsky, S., 2003. Evaluation of
1023 ecosystem dynamics, plant geography and terrestrial carbon cycling in the LPJ
1024 dynamic global vegetation model. *Global Change Biology* 9, 161-185.

1025 Smith, B., Prentice, I.C., Sykes, M.T., 2001. Representation of vegetation dynamics
1026 in the modelling of terrestrial ecosystems: comparing two contrasting
1027 approaches within European climate space. *Global Ecology and Biogeography* 10,
1028 621-637.

1029 Sperry, John S., 2003. Evolution of water transport and xylem structure.
1030 *International Journal of Plant Sciences* 164, S115-S127.

1031 Swaine, M., Whitmore, T., 1988. On the definition of ecological species groups in
1032 tropical rain forests. *Vegetatio* 75, 81-86.

1033 Ter Braak, C.J., Prentice, I.C., 1988. A theory of gradient analysis. *Advances in*
1034 *Ecological Research* 18, 271-317.

1035 Togashi, H.F., Prentice, I.C., Atkin, O.K., Macfarlane, C., Prober, S., Bloomfield, K.J.,
1036 Evans, B., 2017. Thermal acclimation of leaf photosynthetic traits in an evergreen
1037 woodland, consistent with the co-ordination hypothesis. *Biogeosciences Discuss.*,
1038 <https://doi.org/10.5194/bg-2017-449>, in review, 2017.

1039 Togashi, H.F., Prentice, I.C., Evans, B.J., Forrester, D.I., Drake, P., Feikema, P.,
1040 Brooksbank, K., Eamus, D., Taylor, D., 2015. Morphological and moisture
1041 availability controls of the leaf area-to-sapwood area ratio: analysis of
1042 measurements on Australian trees. *Ecology and Evolution* 5, 1263-1270.

1043 Turner, I.M., 2001. *The Ecology of Trees in the Tropical Rain Forest*. Cambridge
1044 University Press.

1045 Tyree, M.T., Ewers, F.W., 1991. The hydraulic architecture of trees and other
1046 woody plants. *New Phytologist* 119, 345-360.

1047 van Bodegom, P.M., Douma, J.C., Verheijen, L.M., 2014. A fully traits-based
1048 approach to modeling global vegetation distribution. *Proceedings of the National*
1049 *Academy of Sciences* 111, 13733.

1050 Verheijen, L., Brovkin, V., Aerts, R., Bönish, G., Cornelissen, J., Kattge, J., Reich, P.,
1051 Wright, I., Van Bodegom, P., 2013. Impacts of trait variation through observed

1052 trait-climate relationships o performance of a representative Earth System
1053 Model: a conceptual analysis. *Biogeosciences* 10, 5497-5515.

1054 Wang, H., Harrison, S.P., Prentice, I.C., Yang, Y., Bai, F., Togashi, H.F., Wang, M.,
1055 Zhou, S., Ni, J., 2018. The China Plant Trait Database: toward a comprehensive
1056 regional compilation of functional traits for land plants. *Ecology* 99, 500-500.

1057 Wang, H., Prentice, I.C., Keenan, T.F., Davis, T.W., Wright, I.J., Cornwell, W.K.,
1058 Evans, B.J., Peng, C., 2017. Towards a universal model for carbon dioxide uptake
1059 by plants. *Nature Plants* 3, 734-741.

1060 Warton, D.I., Wright, I.J., Falster, D.S., Westoby, M., 2006. Bivariate line - fitting
1061 methods for allometry. *Biological Reviews* 81, 259-291.

1062 Weerasinghe, L.K., Creek, D., Crous, K.Y., Xiang, S., Liddell, M.J., Turnbull, M.H.,
1063 Atkin, O.K., 2014. Canopy position affects the relationships between leaf
1064 respiration and associated traits in a tropical rainforest in Far North Queensland.
1065 *Tree Physiology* 34, 564-584.

1066 Whitehead, D., Edwards, W.R.N., Jarvis, P.G., 1984. Conducting sapwood area,
1067 foliage area, and permeability in mature trees of *Picea sitchensis* and *Pinus*
1068 *contorta*. *Canadian Journal of Forest Research* 14, 940-947.

1069 Whitmore, T., 1982. On pattern and process in forests. In: Newman, E. I. (ed.),
1070 *The plant community as a working mechanism*. pp. 45-59. Blackwell, Oxford.

1071 Wickham, H., 2010. *ggplot2: Elegant Graphics for Data Analysis*. Springer.

1072 Woodward, F.I., 1987. *Climate and Plant Distribution*. Cambridge University
1073 Press.

1074 Wright, I.J., Reich, P.B., Westoby, M., Ackerly, D.D., Baruch, Z., Bongers, F.,
1075 Cavender-Bares, J., Chapin, T., Cornelissen, J.H.C., Diemer, M., Flexas, J., Garnier,
1076 E., Groom, P.K., Gulias, J., Hikosaka, K., Lamont, B.B., Lee, T., Lee, W., Lusk, C.,
1077 Midgley, J.J., Navas, M.-L., Niinemets, U., Oleksyn, J., Osada, N., Poorter, H., Poot, P.,
1078 Prior, L., Pyankov, V.I., Roumet, C., Thomas, S.C., Tjoelker, M.G., Veneklaas, E.J.,
1079 Villar, R., 2004. The worldwide leaf economics spectrum. *Nature* 428, 821-827.

1080 Yang, Y. , Wang, H. , Harrison, S.P., Prentice, I.C., Wright, I.J., Peng, C., Lin, G., 2018.
1081 Quantifying leaf - trait covariation and its controls across climates and biomes.
1082 *New Phytologist* (online). doi:10.1111/nph.15422

1083 Zhou, S., Duursma, R.A., Medlyn, B.E., Kelly, J.W. and Prentice, I.C., 2013. How
1084 should we model plant responses to drought? An analysis of stomatal and non-
1085 stomatal responses to water stress. *Agricultural and Forest Meteorology* 182,
1086 204-214.

1087